# Sustainable processing of Europe's low-grade sulphidic and lateritic nickel/cobalt ores and tailings into battery-grade metals
# (ENICON)

## Deliverable D2.4

This project has received funding from the European Union's EU
Framework Programme for Research and Innovation Horizon
Europe under Grant Agreement No 101058124
[https://enicon-horizon.eu/](https://enicon-horizon.eu/)

Public

Authors:

Brecht Dewulf, KU Leuven

Seyedehmaryam Sadeghi, KU Leuven

Rayco Lommelen, KU Leuven

Rodolfo Marín Rivera, KU Leuven

Koen Binnemans, KU Leuven

Date:

26-11-2024

This project has received funding from the European Union's EU Framework Programme for Research and Innovation Horizon Europe under Grant Agreement No 101058124
https://enicon-horizon.eu/

| | |
|---|---|
| **Deliverable Number** | D2.4 |
| **Deliverable Name** | Technical report on the success of the various unit processes in the HCl-route for 5 distinct ENICON input materials |
| **Due Date of Deliverable** | 30-11-2024 |
| **Actual Submission Date** | |
| **Deliverable Lead Organisation** | KU Leuven |
| **Dissemination Level** | Public |
| **Public Summary enclosed** | No |
| **Work Package** | WP2: "Ni/Co Recovery" |
| **No of Pages** | 48 |
| **Keywords** | cobalt, hydrolytic stripping, leaching, nickel, solvent extraction, SX-assisted carbonation, thermodynamic modelling |
| **In bibliography, this report should be cited as follows:** | Brecht Dewulf, Seyedehmaryam Sadeghi, Rayco Lommelen, Rodolfo Marín Rivera, Koen Binnemans, Technical report on the success of the various unit processes in the HCl-route for 5 distinct ENICON input materials. (D2.4) ENICON - Sustainable processing of Europe's low-grade sulphidic and lateritic nickel/cobalt ores and tailings into battery-grade metals, 2024. |

This project has received funding from the European Union's EU Framework Programme for Research and Innovation Horizon Europe under Grant Agreement No 101058124
https://enicon-horizon.eu/

# 1 Executive Summary

This technical report reports on the success of variable unit processes in the HCl-route for 5 different input materials. Research has focused on the following tasks:

- **Task 2.3.1 HCl-leaching and washing of the leach residue, incl. thermodynamic modelling:** leaching performance has been studied on a wide array of ENICON materials, after which 5 materials were selected for further optimisation of the downstream processes.
- **Task 2.3.2 SX process for HCl recovery incl. thermodynamic modelling:** HCl recovery was performed by using the neutral extractant tri-*n*-butyl phosphate (removes both iron(III) and HCl) and the basic extractant tris(ethylhexyl) amine (removes HCl only). The former combines both task 2.3.2 and 2.3.4, and hence intensifies the recovery process, increasing efficiency. Modeling of acid extraction by TBP has been studied intensively, and two papers were published based on these studies.
- **Task 2.3.3 Solution purification of SX raffinate producing a Ni/Co-rich solution for ultra-refining**: depending on the material studied in the flowsheet, cobalt and nickel will need further purification, i.e. cobalt and nickel need to be separated from impurities such as magnesium and calcium. This was studied using Versatic Acid 10 instead of Cyanex 301, since latter extractant is no longer commercially available. The purified nickel- and cobalt-containing aqueous solution is to be used in **Task 3.1 Development of Ni/Co ultra-refining process through Direct Oxide Recovery** and **Task 3.2 Ultra-refining of Ni/Co-intermediate from next-gen' HCl-route in an existing hydro-process**.
- **Task 2.3.4 Chloride-to-oxide conversion and HCl regeneration, incl. thermodynamic modelling**: this includes both the hydrolytic stripping of $FeCl_3$ from aqueous solution to produce hematite and HCl, and the SX-assisted carbonation, transforming $MgCl_2$ and $CaCl_2$ to $MgCO_3$ and $CaCO_3$, respectively, by purging with $CO_2$, while contacting the aqueous solution with tris(ethyl hexyl) amine to extract the formed acid. For the SX-assisted carbonation, a proof-of-concept study has been performed using LiCl instead, while studies on $MgCl_2$ and $CaCl_2$ are still ongoing.

Preliminary flowsheets for five selected materials were developed. These five materials are:

- saprolitic laterite (ENICON028, from Turkey, Euronickel)
- limonitic laterite (ENICON017, from Evia in Greece, Larco)
- Ferronickel (ENICON023, from pyro-processing at Larco, Greece)
- Mixed hydroxide precipitate (ENICON013, MHP, from pyrite tailings at Kevitsa in Finland, Boliden)
- Mixed sulphide precipitate (ENICON014, MSP, from pyrite tailings at Kevitsa in Finland, Boliden)

These materials were chosen based on their industrial relevance and the feasibility to apply the proposed HCl-route. Screening experiments during the HCl-leaching task showed that the Ni/Co-rich intermediates and laterite ores could provide the most concentrated pregnant leach solutions, which is both technically and economically advantageous for downstream processing using solvent extraction. Moreover, the envisioned HCl-route can provide clear advantages, both techno-economic and environmental, with regard of the current state-of-the-art for (limonitic) laterite processing, i.e. high-pressure acid leaching. The sulphidic concentrates and tailings, on the other hand, were generally low-grade, and leaching was complicated by excessive $H_2S$ formation. Moreover, leaching yields were generally low when trying to work at higher solid-to-liquid ratios. As to the sulphidic concentrates, the pyrometallurgical processes currently applied in industry to treat these materials are already of such efficiency for nickel recovery, that a new, HCl-based hydrometallurgical flowsheet would not be able to compete in terms of economic and environmental efficiency. The only improvement to be obtained from the HCl-route, would be enhanced recovery of cobalt. Hence, it was concluded with the industrial partners, not to pursue this path.

The experimental work in Task 2.3 (leaching, solvent extraction, hydrolytic distillation) was supported by thermodynamic modelling using the OLI Mixed-Solvent Electrolyte (OLI-MSE) thermodynamic framework. The developed thermodynamic model was able to calculate the boundary conditions, at which the leaching and/or extraction yields would still be optimal.

As to the leaching, for all above-mentioned materials, various leaching conditions were optimised: HCl concentration, solid-to-liquid ratio, time, temperature, and, if applicable, $H_2O_2$ concentration. Leaching for the selected materials was performed on a slightly larger scale (900 mL), to provide the pregnant leach solutions to be used for solvent extraction optimisation.

Based on the leachate composition, the various solvent extraction unit processes were optimised, i.e. iron (and HCl) removal by tri-*n*-butyl phosphate, recovery of excess HCl by tris(2-ethylhexyl) amine (TEHA), and recovery of cobalt and nickel by Versatic Acid 10, which leaves only impurities such as magnesium and calcium chloride in the aqueous solution. The parameters that were studied during solvent extraction tests (extraction-scrubbing-stripping) were, depending on the extractant system: extractant concentration, diluent type, modifier concentration, organic-to-aqueous volume ratio, temperature, time, pH.

With the *Twelve Principles of Circular Hydrometallurgy* in mind,[1] further recovery of HCl from the impurity waste streams containing $FeCl_3$, $MgCl_2$ and $CaCl_2$ were investigated. Experiments and thermodynamic calculations for the recovery of HCl from $FeCl_3$ solutions by hydrolytic distillation were performed. Furthermore, proof-of-principle tests on LiCl solutions were carried out prior to tests with $MgCl_2$ and $CaCl_2$ solutions, to test if carbonation of these salts, combined with solvent extraction using tris(2-ethylhexyl) amine can successfully recover most HCl from aforementioned salts.

Finally, the preliminary technical flowsheets presented here will lay the foundation of the work to be performed in **Task 2.3.5 Process integration and mini-pilot level demonstration**, which will be presented in the future Deliverable **D2.5 Final report on the pilot-level demonstration of next-generation HCl-route**. Present report also informs about the decision on the selection of the 3 most appropriate input materials for the mini-pilot demonstration (Milestone 11).

# 2 Table of Contents

This project has received funding from the European Union's EU
Framework Programme for Research and Innovation Horizon
Europe under Grant Agreement No 101058124
https://enicon-horizon.eu/

# 3 List of abbreviations

| | |
|---|---|
| %*E* | extraction efficiency (in %) |
| %*Str* | stripping efficiency (in %) |
| CCES | counter-current extraction simulation |
| FeNi | ferronickel |
| HPAL | high-pressure acid leaching |
| KPI | key performance indicator |
| MHP | mixed hydroxide precipitate |
| MSP | mixed sulphide precipitate |
| O:A | organic-to-aqueous (volume phase ratio) |
| ORP | oxidation-reduction potential |
| PLS | pregnant leach solution |
| S/L | solid-to-liquid ratio |
| SX | solvent extraction |
| TBP | tri-*n*-butyl phosphate |
| TEHA | tris(2-ethylhexyl) amine |
| TisoOA | tri-*iso*-octyl amine |
| TOA | tri-*n*-octyl amine |

## 4 Introduction

Cobalt and nickel are essential for the green transition, especially due to their use in Ni/Co-based lithium batteries. With a steadily increasing demand for such batteries for electric mobility and energy storage, the demand for nickel and cobalt is expected to increase rapidly in the coming years. Currently, Europe takes up only a minor part of the global battery supply chain and most nickel and cobalt mining and refining are taking place in the Democratic Republic of Congo (cobalt mining) and Indonesia (nickel mining and refining), with an ever-increasing role for China across all stages of the value chain.

In order to increase the resilience of the European industrial value chains, it is essential to concentrate our efforts in mining and refining nickel and cobalt from existing domestic primary and secondary resources, such as sulphidic Ni/Co ores, limonitic and saprolitic laterites, ferronickel from pyro-processing of laterites, mixed hydroxide or sulphide precipitates (MHP/MSP), … However, this should be accomplished in an eco-friendly way, reducing the carbon footprint and reducing waste streams. In ENICON, this is realised by a new, low-pressure, low-temperature hydrometallurgical approach using a HCl-based route, with a special focus on *circular hydrometallurgy*,[1] which reduces the consumption of chemicals and avoids the generation of vast amounts of waste. This is a green alternative for the High-Pressure Acid Leaching (HPAL) process, which is currently the mainstream process for laterite processing in Indonesia. The resource- and energy-intensive, linear HPAL process relies on sulphuric acid leaching at high temperatures and pressures, resulting in a large carbon footprint.[2–4] The HCl process to be developed, as shown in Figure 1, is mainly situated in Work Package 2 and includes (1) atmospheric low-temperature leaching, (2) three solvent extraction (SX) process steps, i.e. iron removal by tri-*n*-butyl phosphate (TBP), excess HCl recovery by tris(2-ethylhexyl) amine (TEHA) and recovery of cobalt and nickel by Versatic Acid 10, (3) recovery of HCl from the removed $FeCl_3$ by hydrolytic distillation, (4) recovery of HCl by SX-assisted carbonation of $MgCl_2$ and $CaCl_2$ left in the raffinate solution after cobalt and nickel recovery. Not necessarily all process steps will be needed, as it will depend on the composition of the studied input streams. The purified Ni/Co solution that is produced in the process is subsequently transferred to WP3, for the ultra-refining to produce battery-grade cobalt and nickel, i.e. *Task 3.1 Development of Ni/Co ultra-refining process through Direct Oxide Recovery* and *Task 3.2 Ultra-refining of Ni/Co-intermediate from next-gen' HCl-route in an existing hydro-process*.

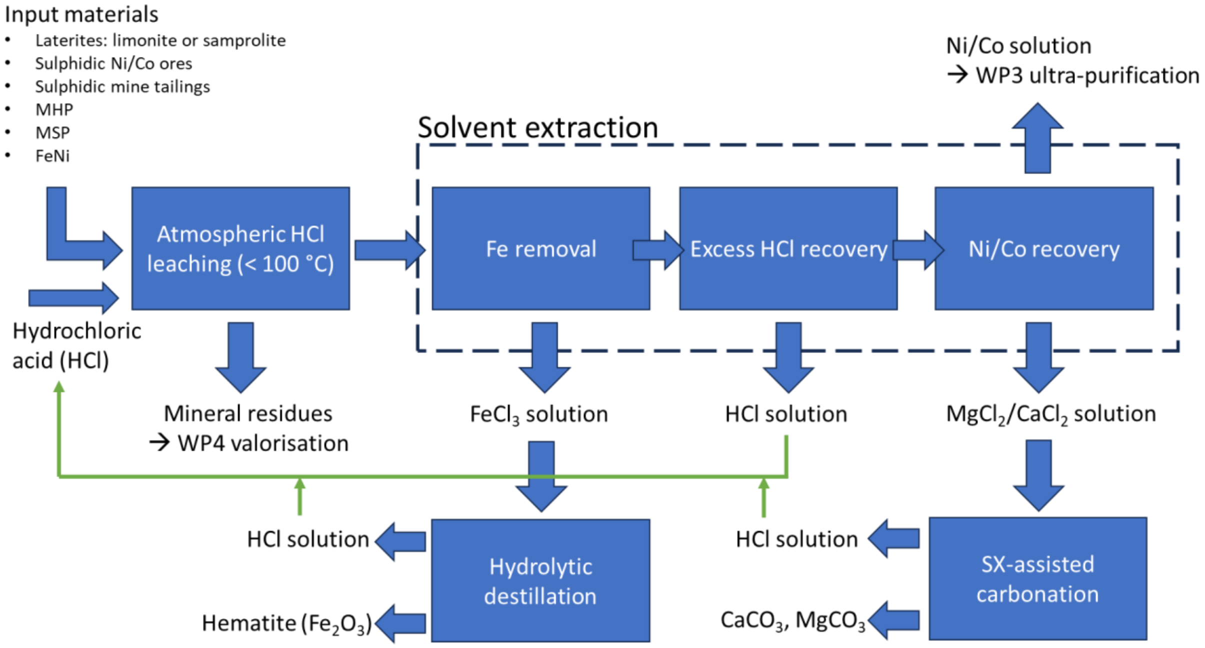

**Figure 1.** General overview of the Task 2.3 flowsheet

This project has received funding from the European Union's EU Framework Programme for Research and Innovation Horizon Europe under Grant Agreement No 101058124
https://enicon-horizon.eu/

## 4.1 Goal of the work and link of this deliverable to ENICON objectives

The work presented in this report describes the technical feasibility of abovementioned process flowsheet based on bench-scale optimisation experiments carried out on 5 different materials. These materials were chosen based on their industrial and scientific relevance. The research conducted within Task 2.3 should eventually lead to comprehensive, material-tailored flowsheets, which include all of the hydrometallurgical unit processes described in the Task. A detailed task-by-task description of the goals of the performed research can be found in the Executive summary.

The main objective of this work, as stated in the Grant Agreement, is *to develop a flexible, new HCl-based route (enhanced leaching, purification & direct oxide recovery) as an alternative to state-of-the-art processing routes for sulphide concentrates (pyro) & laterite ores (pyro & HPAL). The new HCl route, which produces battery-grade Ni and Co precursors, can be extended/adapted for processing (1) FeNi from laterites, (2) MSP (MHP) from bioleaching/oxidative leaching of Co-rich pyrite tailings, (3) carbonated Ni/Co-containing silicate tailings. (Objective 4 – WP2&3)*

KPI's related to this objective are (1) *purity of Ni/Co(aq.) solution from metal purification: Ni+Co concentration > 42 wt% (in derived MHP) & > 55 wt% (in derived MSP) (for downstream processing in state-of-the-art hydro-process);* and (2) *purity of Ni and Co > 99.5 wt% (i.e. battery-grade quality, for conversion into $NiSO_4$ and $CoSO_4$ precursors)*. The latter KPI value is related to the Ni and Co obtained in WP3, as the only output of WP2 are either mixed Ni/Co solutions or MHP, for downstream purification. Hence, the first KPI is of interest in this report.

# 5 Experimental conditions

## 5.1 Chemical analysis of the materials

To properly quantify the elemental content of the laterite sample, the milled laterite was completely digested by an acid mixture of HF, HCl, and $HNO_3$ with a ratio of 3:1:3, respectively, under microwave irradiation. Aliquots of 100 mg of samples were transferred in polytetrafluoroethylene (PTFE) microwave vessels with 3 mL of $HNO_3$, 3 mL of HF, and 1 mL of HCl. The samples were then digested in a microwave reactor (CEM Mars 6) at 180 °C for 15 minutes with a temperature ramp of 7 °C/minute. The solutions were let to cool down to room temperature naturally. Further, the samples were neutralised using 20 mL of a 1.2 M boric acid solution and again temperature treated under microwave irradiation at 170 °C for 10 minutes with a ramp of 11 °C/minute. The vessels were allowed to cool down to room temperature and visually checked for any solid residues.

In the case of FeNi, MSP and MHP aliquots of 100 mg of samples were digested using aqua regia ($HNO_3$:HCl = 1:3) under microwave irradiation at 200 °C for 10 minutes with a ramp temperature of 10 °C/minute. Finally, the samples were measured by ICP-OES for metal quantification. The samples preparation for ICP-OES involved a dilution in HCl (10 vol%).

## 5.2 Leaching procedure

In this work, two laterites—one limonite ENICON017, and one saprolite ENICON028— ferronickel ENICON023, MHP ENICON013 and MSP ENICON014 were subjected to acid leaching using HCl. All the bench-scale experiments for laterite were performed on crushed samples with an average particle size of ≤500 µm while for mini-pilot scale original laterite used without any pretreatment.

In general, to define an optimal leaching system, the impact of different variables involved in the acid leaching, i.e. temperature, liquid/solid ratio, acid concentration and concentration of $H_2O_2$ as an oxidant (if any) was evaluated. Typical experiments were carried out in screw-cap closed glass vials of 40 mL volume. Firstly, a predefined amount of original or milled sample was precisely weighed and added to the vial, followed by the addition of the HCl and $H_2O_2$ if it was required. The vials were placed in the heating block, and the mixture was heated up to the target level for the leaching time mainly varied between 1-3 hours. Magnetic stirring at 500 rpm was used to ensure sufficient mixing and solid-liquid contact during the entire leaching time. After the leaching was completed, the slurries were firstly filtered to separate the PLS from the residue. The residues were washed with sufficient amount of milli-Q water. All leaching tests were conducted in triplicates to assess the repeatability of the experimental results, and the observed error fell within the 10% range.

The optimised leaching conditions for each stream were used for scale-up using a 1L reactor, and the kinetics of the leaching reaction, as well as the ORP and pH of the PLS, were monitored during the process. For FeNi and MSP, the ORP of the solution was kept above 350 mV by the stepwise addition of $H_2O_2$ to prevent the formation of $H_2$ and $H_2S$, respectively.

## 5.3 Solvent extraction procedure

Batch–scale solvent extraction experiments were performed on the pregnant leach solution (PLS), prepared through leaching of the selected materials, i.e. limonite ENICON017, saprolite ENICON028, ferronickel ENICON023, MHP ENICON013 and MSP ENICON014. Depending on the PLS composition, three distinct solvent extraction processes were studied: extraction of iron(III)chloride by TBP, extraction of HCl by TEHA and extraction of cobalt and nickel by Versatic Acid 10.

In case of the ferronickel PLS, addition of a small excess (25 mol% above stoichiometric amount) of $H_2O_2$ was added to oxidise Fe(II) to Fe(III), prior to solvent extraction. The reaction was followed via UV/Vis spectroscopy and ICP–OES. A sample would be diluted 50 times in milliQ water, after which 20 µL of this dilution would be mixed with 1 mL of buffer solution (5 mol $L^{-1}$ NaOH + 6 mol $L^{-1}$ acetic acid), 5 mL of an aqueous 1,10-phenanthroline solution (2 wt%) and 3.98 mL milliQ water. The UV-Vis absorption band at 511 nm, corresponding with the Fe(II)-phenanthroline complex was used for quantification.

The extraction of iron(III)chloride was performed by contacting undiluted, water–presaturated TBP with the PLS. Both phases were contacted for 60 min at 500 rpm in 20 mL glass vials . Depending on the experiment, the organic–to–aqueous (O:A) volume ratios would be varied, while the total sample volume (O+A) remained 6 mL. Stripping of the loaded organic phase was carried out using milliQ water at room temperature, stirred at 600 rpm for 60 min on a total volume of 6 mL at variable O:A ratios. After each experiment, argentometric titration and elemental analysis via ICP–OES of was carried out on the aqueous phases

The extraction of excess HCl was performed using a 10 – 50 vol% TEHA diluted in aliphatic, mixed aliphatic-aromatic or fully aromatic diluents, i.e. Shellsol D70, Shellsol 2046 and Shellsol A150, respectively. Addition of modifiers (1-octanol, 2-octanol or 1-decanol, 5 – 10 vol%) was tested as well. The extraction was performed by contacting equal volumes of aqueous and organic phases (3 mL : 3 mL) for 60 min at 500 rpm, room temperature. The organic phases were then subjected to a stripping step using milliQ water, at 60 °C and O:A = 1:1 – 2:1, for 60 min at 500 rpm.

Cobalt and nickel extraction was performed by Versatic Acid 10. The PLS used for the optimisation experiments was generated by contacting the original PLS (laterite PLS) twice with fresh, undiluted TBP, in order to extract all Fe(III) and most HCl. The pH was first adjusted to 5.5 (unless stated differently). Any precipitate formed during this operation is filtered off. The resulting adjusted PLS is contacted at O:A = 1:1 with 40 vol% Versatic Acid 10, for 5 min. pH is then checked and adjusted to create a pH isotherm. After pH adjustment, the solutions are stirred for another 30 min, and final pH is measured. After each experiment, elemental analysis via ICP–OES of was carried out on the aqueous phases.

The results of solvent extraction experiments are presented as extraction efficiency (%E) and stripping efficiency (%Str). Extraction efficiency, or percentage extraction, is presented in Equation 1, with $C_{i,E}$ the initial concentration of the metal or acid in the feed solution before extraction, and $C_{f,E}$ is the concentration of the metal or acid in the raffinate after the extraction experiment. The stripping efficiency, or percentage stripping, was calculated according to Equation 2, where $C_{f,Str}$ is the concentration of metal or acid in the strip raffinate.

$$\%E = \frac{C_{i,E} - C_{f,E}}{C_{i,E}} \cdot 100\% \tag{1}$$

$$\%Str = \frac{C_{f,Str}}{C_{i,E} - C_{f,E}} \cdot 100\% \tag{2}$$

## 5.4 Hydrolytic stripping

This project has received funding from the European Union's EU Framework Programme for Research and Innovation Horizon Europe under Grant Agreement No 101058124
https://enicon-horizon.eu/

A setup (Figure 2) has been built to allow distillation at 180 °C with continuous water addition to avoid drying out the boiling solution. For safety, any non-condensed HCl will be captured in washing bottles with NaOH solution and an HCl detector is always present. This setup has been used to produce HCl from $FeCl_3$ and $AlCl_3$ solutions and mixtures thereof in a range from 0 to 4 mol $L^{-1}$ of salt. ICP-OES (PerkinElmer Avio 500) has been used to determine the Fe and Al concentrations in the feed, solution after boiling, and condensate. HCl content in the condensate was determined with an automated acid-base titration (Mettler-Toledo titrator T5 Excellence, and an InMotion Flex autosampler) with 0.1 mol $L^{-1}$ KOH. Volumes as the leftover solution after distillation and of the condensate were determined with a volumetric flask. The amount of water added to the system at any moment was recorded based on a calibrated peristaltic pump. This allows to calculate conversions based on the system's total volume and the condensate's HCl content.

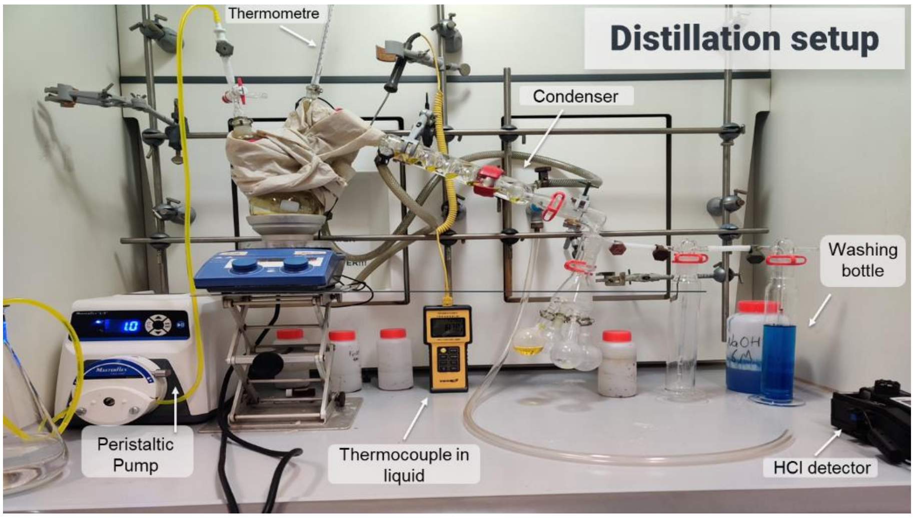

**Figure 2.** Hydrolytic distillation setup

### 5.5 *SX-assisted carbonation*

A synthetic solution was prepared from the salt lithium chloride (LiCl, ≥ 95% Chem-lab) with a lithium concentration of 30 g $L^{-1}$. Tri-*n*-octyl amine (TOA, BLD Pharmatech Ltd., 97%), tris(2-ethylhexyl) amine (TEHA, Sigma Aldrich, ≥ 97%) and tri-*iso*-octyl amine ($T_{iso}OA$, BLD Pharmatech Ltd., 98%) were investigated as extractants, whereas 1-octanol (Thermo Scientific, 99%) and Shellsol D70 (Shell Chemicals, 100% aliphatic diluent) were studied as diluents.

The lithium conversion (into carbonate) and the acid regeneration from the lithium-based salt was evaluated in two consecutive experimental processes, according to the diagram depicted in Figure 3: (1) simultaneous acidity extraction and mineral carbonation from the initial aqueous solution, and (2) subsequent acid regeneration by stripping with water the loaded organic phase. Three different organic-to-aqueous (O:A) ratios (1, 3 and 6) were evaluated during the extraction/carbonation stage, whereas stripping experiments were carried out with the addition of milli-Q water with an O:A ratio of 0.3 and at 60 ˚C. All the experiments lasted for 30 minutes.

This project has received funding from the European Union's EU Framework Programme for Research and Innovation Horizon Europe under Grant Agreement No 101058124
https://enicon-horizon.eu/

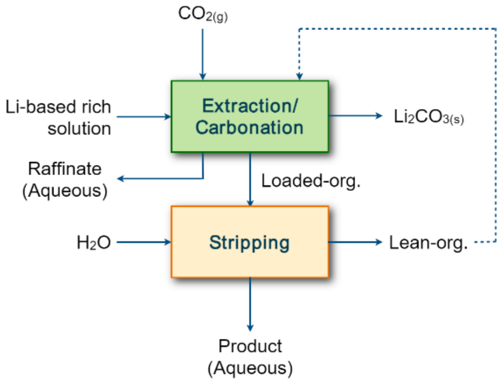

**Figure 3.** Flow sheet for the coupled reaction of mineral carbonation and solvent extraction process (SX-assisted carbonation).

Extraction/carbonation experiments were carried out in a cylindrical reactor of 100 mL capacity (total volume of solution: 60 mL) with continuous agitation. $CO_2$ gas (99.998 %, Air Liquid) was introduced continuously at a flow rate, $Q_{CO2}$, of 40–50 mL/min, which was controlled with a flow meter. The solutions after extraction/carbonation were filtered using filter paper (pore size 0.45 µm) at the end of the experiment, for later on to be poured into separation funnels of 100 mL capacity. The pH of the aqueous phase was measured after being separated from the organic phase, and diluted with 2 vol% $HNO_3$ for Inductively Couple Plasma Optical Emission Spectroscopy (ICP-OES, PerkinElmer Optima 8300) analysis for lithium. The corresponding amount of lithium in solution, $\alpha$% (in wt%) was calculated according to Equation 3:

$$\alpha(\%) = \frac{Amount\ of\ metal\ in\ solution\ after\ extraction/carbonation}{Initial\ amount\ of\ metal} \times 100 \qquad (3)$$

The yield of lithium conversion (in wt%) was calculated according to Equation 4:

$$Li\ conversion = 100 - \alpha(\%) \qquad (4)$$

The obtained carbonated product was dried and studied by X-ray powder diffraction (XRD, Bruker D2 Phaser).

Stripping experiments were carried out with milli-Q water at 60 ˚C in vials of 40 mL capacity with continuous agitation and lasted 30 min. The solutions after stripping were poured into separation funnels of 100 mL capacity. The pH of the aqueous phase was measured after being separated from the organic phase, and diluted with 2 vol% $HNO_3$ for ICP-OES analysis for lithium.

The HCl concentration was determined by stoichiometry from the chloride ion ($Cl^-$) concentration, which was determined by titration (Metter-Toledo T5 automatic titrator) with 0.05 mol $L^{-1}$ $AgNO_3$ as neutralisation reagent.

This project has received funding from the European Union's EU Framework Programme for Research and Innovation Horizon Europe under Grant Agreement No 101058124
https://enicon-horizon.eu/

# 6 Results

## 6.1 Thermodynamic modelling

The OLI Mixed-Solvent Electrolyte (OLI-MSE) thermodynamic framework version 11.0 of OLI Systems Inc. (Parsippany NJ) was used to model the leaching behaviour of Ni/Co ores, concentrates, intermediates and tailings and the solvent extraction of HCl and Fe(III) by TBP using the OLI Studio 11, OLI Databook 11, and OLI Chemistry Wizard 11 software packages of OLI Systems Inc. (Parsippany NJ).[5,6] These are commercial software packages that allow users to build their own thermodynamic model and database. The thermodynamic framework can describe the behavior of electrolytes and non-electrolytes in mixed-solvent systems (mixtures of aqueous and organic solvents). Thus, it is also suited to calculate the complete liquid–liquid equilibrium (LLE) that describes the solvent extraction process of acids and Fe(III) by TBP. More information about the thermodynamic framework can be found in the papers that have been published as a result of the ENICON project: Lommelen and Binnemans (2023) and Lommelen *et al*. (2024).[7,8] An important remark: these calculations represent the thermodynamic equilibrium, they do not take kinetics into account. Thus, leaching conditions are minimum conditions needed for quantitative recovery of the metals of interest (Ni and Co). Certainly for $H_2O_2$, which auto-decomposes, the reaction times and process conditions can greatly influence the percentage of $H_2O_2$ that is actually consumed to oxidise the metals.

Thermodynamic modelling was performed for the 5 distinct flowsheets described in this report: limonite ENICON017, saprolite ENICON028, MHP ENICON013, MSP ENICON014 and FeNi ENICON023. Since the approach for modelling is identical for each of the materials, it was chosen to only focus on the modelling of leaching and solvent extraction for the limonitic laterite ENICON017, to make the discussion more concise. The leaching analysis was performed at different acid concentrations to see what effect the excess acid content has on the downstream TBP steps. Without considering kinetics, 425 mL of a 5 mol $L^{-1}$ HCl solution is enough to leach 100 g of laterite 017 (Figure 4). This entails 2.125 moles of HCl per 100 g of solid. Further processing of this leachate seems difficult due to Fe(III) hydrolysis in the subsequent TBP SX process (Figure 5). The little free acid in the leachate obtained using above mentioned parameters is extracted before Fe(III) extraction, which leads to Fe(III) and maybe Ni-Fe precipitation. The calculations seem to suggest that at least an equimolar amount of free acid and dissolved Fe(III) is necessary to avoid precipitation in the subsequent TBP SX steps. Hence, it seems interesting to aim at leaching conditions that result in a free acid concentration equal to that of the Fe(III) in solutions. This is obtained by leaching 100 g of solids with 525 mL of 5 mol $L^{-1}$ HCl (2.625 moles) at 60 °C (Figure 5). The temperature was chosen arbitrarily as it has no significant impact on the thermodynamic equilibrium. With the slight excess of free HCl in the resulting leachate, efficient extraction of both HCl and Fe(III) by TBP from this leachate is still possible. The model predicts an almost complete co-extraction of HCl with Fe(III) as $[FeCl_4][TBPH^+]$ complexes within 3 counter-current stages using undiluted TBP at room temperature, when an O:A phase ratio of 1.25:1 is selected (Figure 6). The Co+Ni purity, when only considering Fe impurities, increases from 3% to 99.3%, while the raffinate retains 0.07 mol $L^{-1}$ HCl (pH of 1.2). The resulting loaded organic can be stripped at room temperature in a three-stage counter-current stripping step, at an O:A phase ratio of 1.25:1.5 (Figure 7–8). This leaves about 1% of the loaded Fe(III) in the stripped solvent, but this does not significantly impact the SX step upon recycling. The resulting flowsheets calculated for the aforementioned optimal conditions are shown in Figure 9–11 for leaching, extraction and stripping. Hence, according to these calculations, it is possible to avoid an extra solvent extraction circuit for the recovery of excess acid by TEHA.

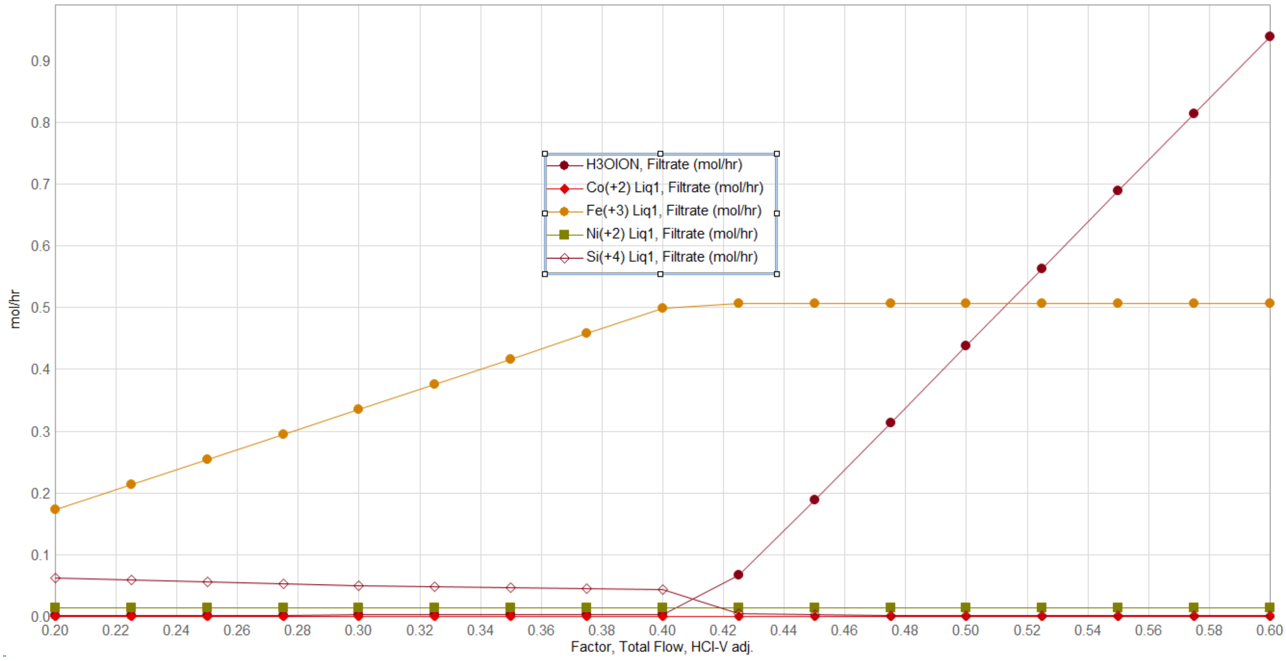

**Figure 4.** Composition of raffinate after leaching and filtration of 100 g ENICON017 (limonite) with a certain volume (x-axis in L) of 5 mol $L^{-1}$ HCl. Only Fe(III), Ni(II), Co(II) and Si(IV) concentrations are shown.

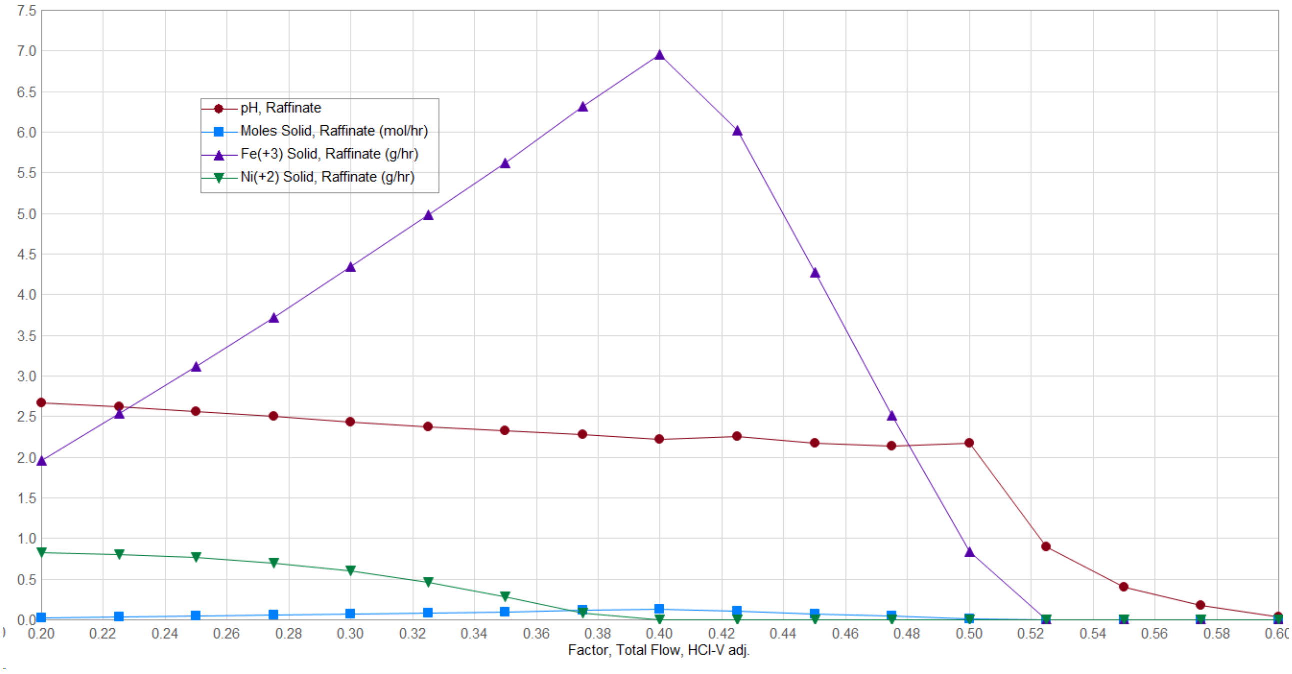

**Figure 5.** Solid raffinate composition and liquid pH with a certain volume (x-axis in L) of 5 mol $L^{-1}$ HCl. Only Fe(III) and Ni(II) concentrations are shown. OLI predicts precipitate formation during SX when the leachate contains less acid than Fe(III).

This project has received funding from the European Union's EU
Framework Programme for Research and Innovation Horizon
Europe under Grant Agreement No 101058124
https://enicon-horizon.eu/

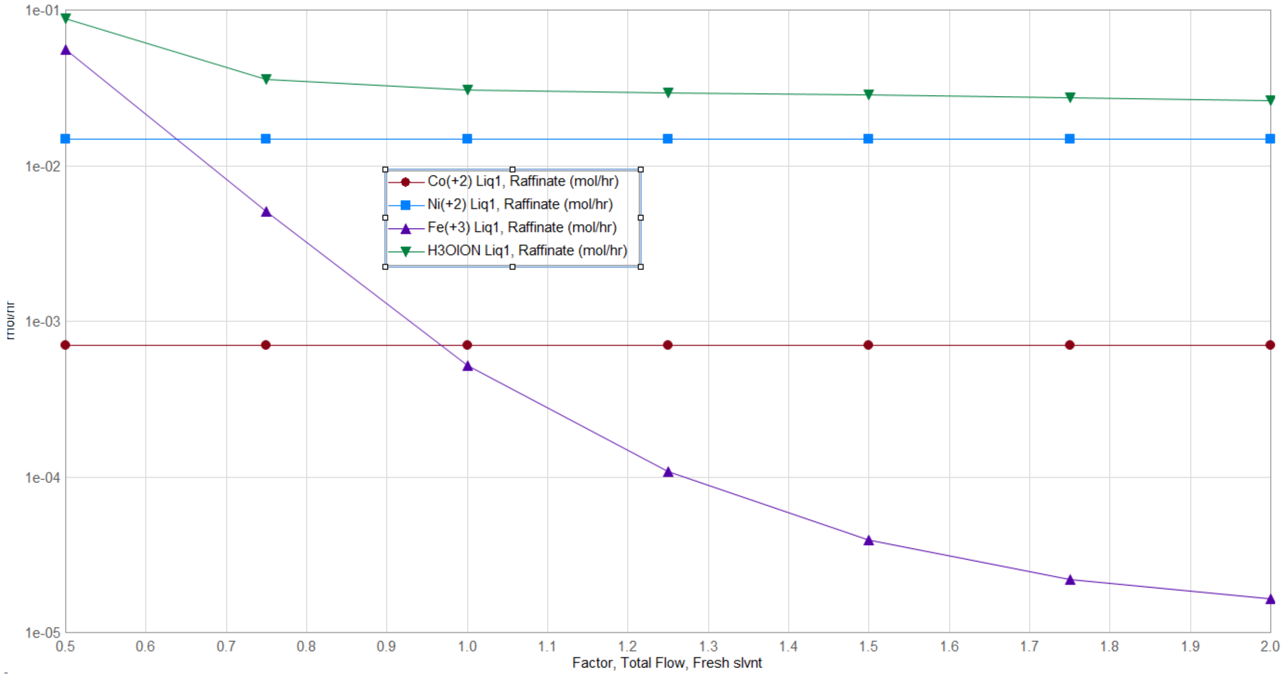

**Figure 6.** Raffinate composition (logarithmic scale, moles) after three-stage counter-current SX with undiluted, recycled TBP. The x-axis shows the volume of the organic phase (in L) used for the extraction. The details of the feed can be found in Figure 10. 1 L solvent results in 97% pure Co+Ni, when only considering Fe impurities. Similarly, this would result in 99.3% purity with 1.25 L of solvent.

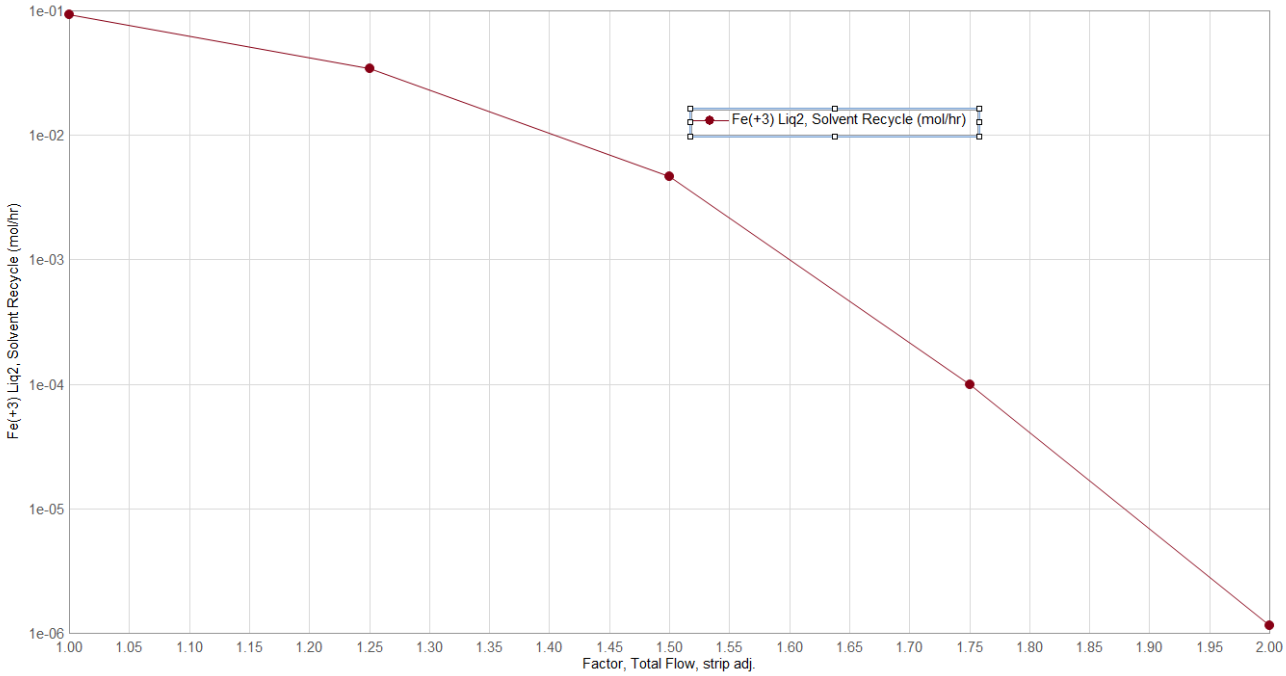

**Figure 7.** Solvent composition (logarithmic scale, moles) after three-stage counter-current stripping of the loaded TBP (1.25 L initial volume) with water, at room temperature. The x-axis shows the volume of water used for stripping (in L). The details of the loaded solvent can be found in Figure 11. 1.25 L water would result in 93% Fe stripping, 1.5 L in 99% stripping, and 1.75 L in 99.98% stripping.

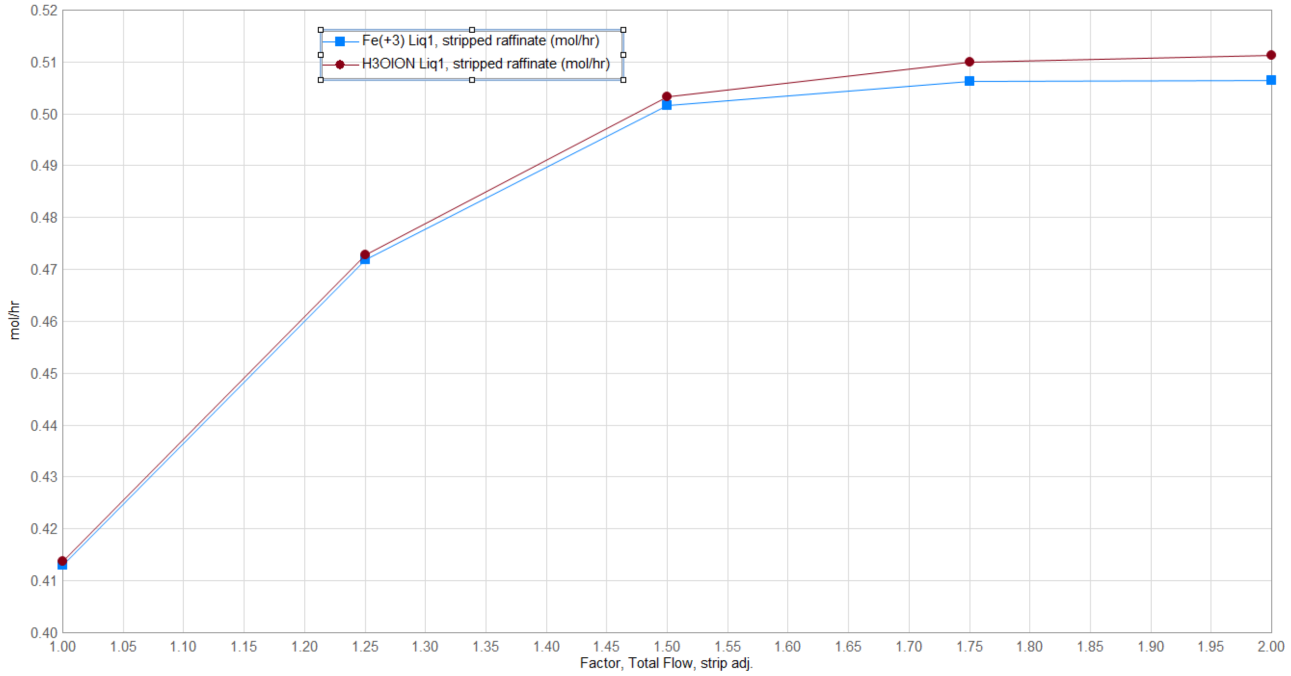

**Figure 8.** Stripping raffinate composition (moles) after three-stage counter-current stripped of the loaded TBP (1.25 L initial volume) with water at room temperature. The x-axis shows the initial volume of water (in L). The details of the loaded solvent can be found in Figure 11.

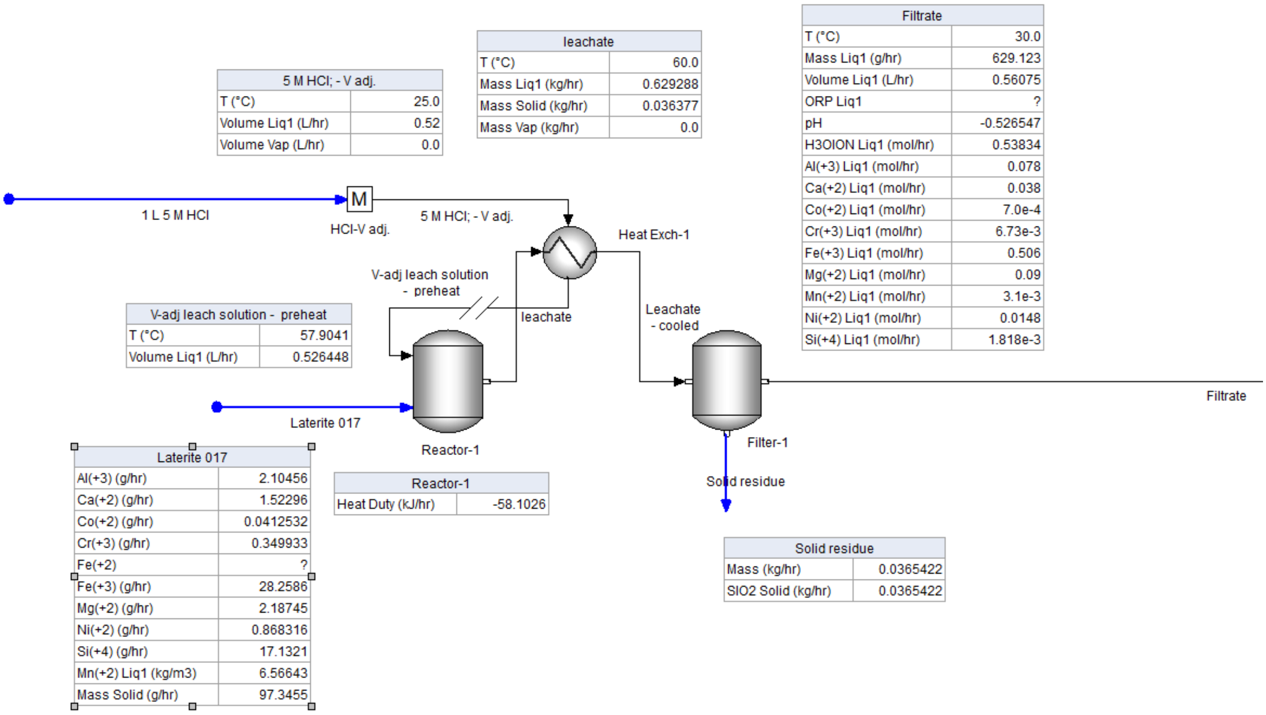

| leachate | |
|---|---|
| T (°C) | 60.0 |
| Mass Liq1 (kg/hr) | 0.629288 |
| Mass Solid (kg/hr) | 0.036377 |
| Mass Vap (kg/hr) | 0.0 |

| Filtrate | |
|---|---|
| T (°C) | 30.0 |
| Mass Liq1 (g/hr) | 629.123 |
| Volume Liq1 (L/hr) | 0.56075 |
| ORP Liq1 | ? |
| pH | -0.526547 |
| H3OION Liq1 (mol/hr) | 0.53834 |
| Al(+3) Liq1 (mol/hr) | 0.078 |
| Ca(+2) Liq1 (mol/hr) | 0.038 |
| Co(+2) Liq1 (mol/hr) | 7.0e-4 |
| Cr(+3) Liq1 (mol/hr) | 6.73e-3 |
| Fe(+3) Liq1 (mol/hr) | 0.506 |
| Mg(+2) Liq1 (mol/hr) | 0.09 |
| Mn(+2) Liq1 (mol/hr) | 3.1e-3 |
| Ni(+2) Liq1 (mol/hr) | 0.0148 |
| Si(+4) Liq1 (mol/hr) | 1.818e-3 |

| 5 M HCl; - V adj. | |
|---|---|
| T (°C) | 25.0 |
| Volume Liq1 (L/hr) | 0.52 |
| Volume Vap (L/hr) | 0.0 |

| V-adj leach solution - preheat | |
|---|---|
| T (°C) | 57.9041 |
| Volume Liq1 (L/hr) | 0.526448 |

| Laterite 017 | |
|---|---|
| Al(+3) (g/hr) | 2.10456 |
| Ca(+2) (g/hr) | 1.52296 |
| Co(+2) (g/hr) | 0.0412532 |
| Cr(+3) (g/hr) | 0.349933 |
| Fe(+2) | ? |
| Fe(+3) (g/hr) | 28.2586 |
| Mg(+2) (g/hr) | 2.18745 |
| Ni(+2) (g/hr) | 0.868316 |
| Si(+4) (g/hr) | 17.1321 |
| Mn(+2) Liq1 (kg/m3) | 6.56643 |
| Mass Solid (g/hr) | 97.3455 |

| Reactor-1 | |
|---|---|
| Heat Duty (kJ/hr) | -58.1026 |

| Solid residue | |
|---|---|
| Mass (kg/hr) | 0.0365422 |
| SIO2 Solid (kg/hr) | 0.0365422 |

**Figure 9.** Leaching section of the calculated optimised ENICON017 (limonite) flowsheet.

This project has received funding from the European Union's EU
Framework Programme for Research and Innovation Horizon
Europe under Grant Agreement No 101058124
https://enicon-horizon.eu/

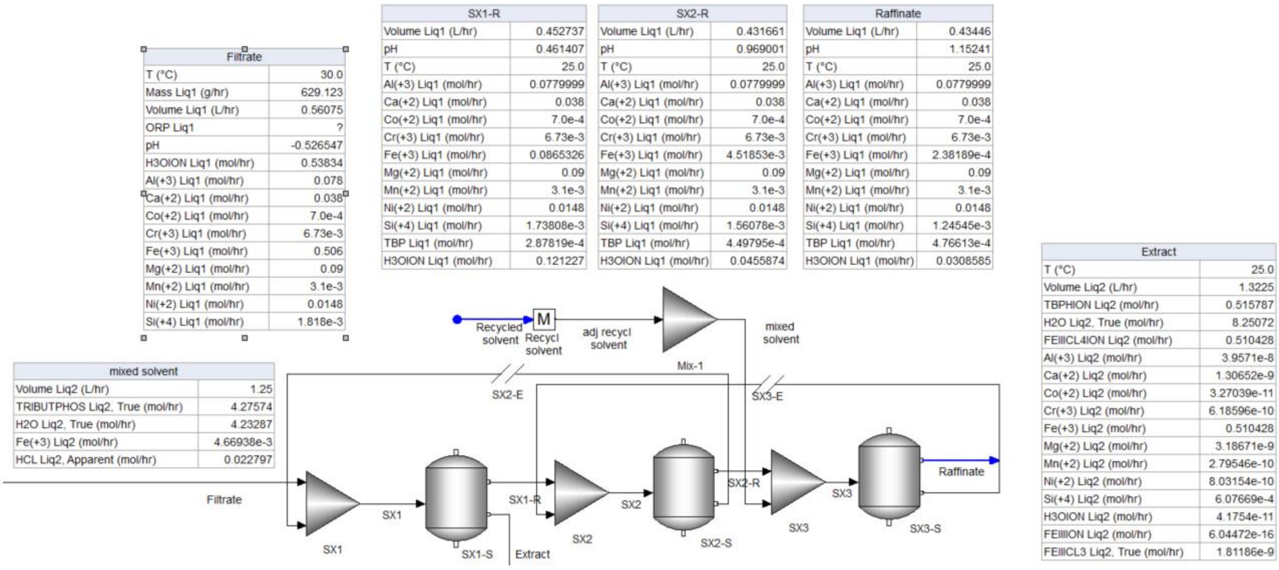

| Filtrate | |
|---|---|
| T (°C) | 30.0 |
| Mass Liq1 (g/hr) | 629.123 |
| Volume Liq1 (L/hr) | 0.56075 |
| ORP Liq1 | ? |
| pH | -0.526547 |
| H3OION Liq1 (mol/hr) | 0.53834 |
| Al(+3) Liq1 (mol/hr) | 0.078 |
| Ca(+2) Liq1 (mol/hr) | 0.038 |
| Co(+2) Liq1 (mol/hr) | 7.0e-4 |
| Cr(+3) Liq1 (mol/hr) | 6.73e-3 |
| Fe(+3) Liq1 (mol/hr) | 0.506 |
| Mg(+2) Liq1 (mol/hr) | 0.09 |
| Mn(+2) Liq1 (mol/hr) | 3.1e-3 |
| Ni(+2) Liq1 (mol/hr) | 0.0148 |
| Si(+4) Liq1 (mol/hr) | 1.818e-3 |

| SX1-R | |
|---|---|
| Volume Liq1 (L/hr) | 0.452737 |
| pH | 0.461407 |
| T (°C) | 25.0 |
| Al(+3) Liq1 (mol/hr) | 0.0779999 |
| Ca(+2) Liq1 (mol/hr) | 0.038 |
| Co(+2) Liq1 (mol/hr) | 7.0e-4 |
| Cr(+3) Liq1 (mol/hr) | 6.73e-3 |
| Fe(+3) Liq1 (mol/hr) | 0.0865326 |
| Mg(+2) Liq1 (mol/hr) | 0.09 |
| Mn(+2) Liq1 (mol/hr) | 3.1e-3 |
| Ni(+2) Liq1 (mol/hr) | 0.0148 |
| Si(+4) Liq1 (mol/hr) | 1.73808e-3 |
| TBP Liq1 (mol/hr) | 2.87819e-4 |
| H3OION Liq1 (mol/hr) | 0.121227 |

| SX2-R | |
|---|---|
| Volume Liq1 (L/hr) | 0.431661 |
| pH | 0.969001 |
| T (°C) | 25.0 |
| Al(+3) Liq1 (mol/hr) | 0.0779999 |
| Ca(+2) Liq1 (mol/hr) | 0.038 |
| Co(+2) Liq1 (mol/hr) | 7.0e-4 |
| Cr(+3) Liq1 (mol/hr) | 6.73e-3 |
| Fe(+3) Liq1 (mol/hr) | 4.51853e-3 |
| Mg(+2) Liq1 (mol/hr) | 0.09 |
| Mn(+2) Liq1 (mol/hr) | 3.1e-3 |
| Ni(+2) Liq1 (mol/hr) | 0.0148 |
| Si(+4) Liq1 (mol/hr) | 1.56078e-3 |
| TBP Liq1 (mol/hr) | 4.49795e-4 |
| H3OION Liq1 (mol/hr) | 0.0455874 |

| Raffinate | |
|---|---|
| Volume Liq1 (L/hr) | 0.43446 |
| pH | 1.15241 |
| T (°C) | 25.0 |
| Al(+3) Liq1 (mol/hr) | 0.0779999 |
| Ca(+2) Liq1 (mol/hr) | 0.038 |
| Co(+2) Liq1 (mol/hr) | 7.0e-4 |
| Cr(+3) Liq1 (mol/hr) | 6.73e-3 |
| Fe(+3) Liq1 (mol/hr) | 2.38189e-4 |
| Mg(+2) Liq1 (mol/hr) | 0.09 |
| Mn(+2) Liq1 (mol/hr) | 3.1e-3 |
| Ni(+2) Liq1 (mol/hr) | 0.0148 |
| Si(+4) Liq1 (mol/hr) | 1.24545e-3 |
| TBP Liq1 (mol/hr) | 4.76613e-4 |
| H3OION Liq1 (mol/hr) | 0.0308585 |

| mixed solvent | |
|---|---|
| Volume Liq2 (L/hr) | 1.25 |
| TRIBUTPHOS Liq2, True (mol/hr) | 4.27574 |
| H2O Liq2, True (mol/hr) | 4.23287 |
| Fe(+3) Liq2 (mol/hr) | 4.66938e-3 |
| HCL Liq2, Apparent (mol/hr) | 0.022797 |

| Extract | |
|---|---|
| T (°C) | 25.0 |
| Volume Liq2 (L/hr) | 1.3225 |
| TBPHION Liq2 (mol/hr) | 0.515787 |
| H2O Liq2, True (mol/hr) | 8.25072 |
| FEIIICL4ION Liq2 (mol/hr) | 0.510428 |
| Al(+3) Liq2 (mol/hr) | 3.9571e-8 |
| Ca(+2) Liq2 (mol/hr) | 1.30652e-9 |
| Co(+2) Liq2 (mol/hr) | 3.27039e-11 |
| Cr(+3) Liq2 (mol/hr) | 6.18596e-10 |
| Fe(+3) Liq2 (mol/hr) | 0.510428 |
| Mg(+2) Liq2 (mol/hr) | 3.18671e-9 |
| Mn(+2) Liq2 (mol/hr) | 2.79546e-10 |
| Ni(+2) Liq2 (mol/hr) | 8.03154e-10 |
| Si(+4) Liq2 (mol/hr) | 6.07669e-4 |
| H3OION Liq2 (mol/hr) | 4.1754e-11 |
| FEIIIION Liq2 (mol/hr) | 6.04472e-16 |
| FEIIICL3 Liq2, True (mol/hr) | 1.81186e-9 |

**Figure 10.** TBP extraction section of the calculated optimised ENICON017 (limonite) flowsheet.

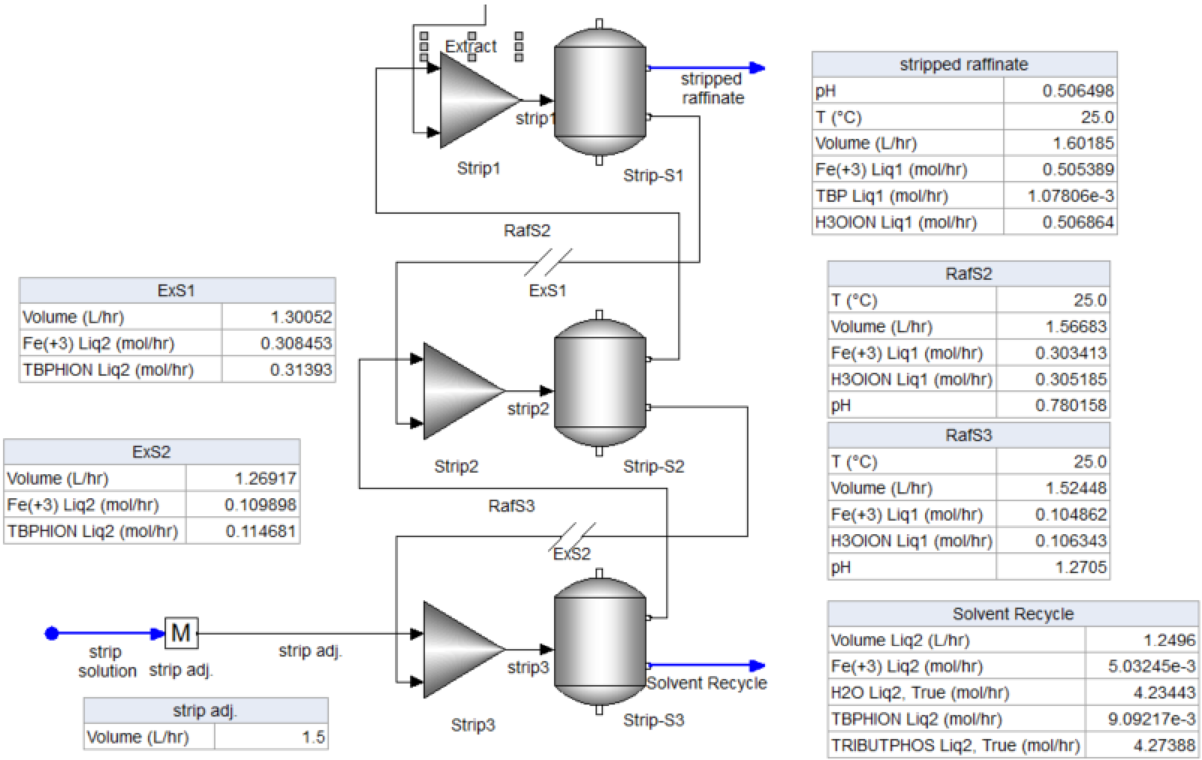

| stripped raffinate | |
|---|---|
| pH | 0.506498 |
| T (°C) | 25.0 |
| Volume (L/hr) | 1.60185 |
| Fe(+3) Liq1 (mol/hr) | 0.505389 |
| TBP Liq1 (mol/hr) | 1.07806e-3 |
| H3OION Liq1 (mol/hr) | 0.506864 |

| ExS1 | |
|---|---|
| Volume (L/hr) | 1.30052 |
| Fe(+3) Liq2 (mol/hr) | 0.308453 |
| TBPHION Liq2 (mol/hr) | 0.31393 |

| RafS2 | |
|---|---|
| T (°C) | 25.0 |
| Volume (L/hr) | 1.56683 |
| Fe(+3) Liq1 (mol/hr) | 0.303413 |
| H3OION Liq1 (mol/hr) | 0.305185 |
| pH | 0.780158 |

| ExS2 | |
|---|---|
| Volume (L/hr) | 1.26917 |
| Fe(+3) Liq2 (mol/hr) | 0.109898 |
| TBPHION Liq2 (mol/hr) | 0.114681 |

| RafS3 | |
|---|---|
| T (°C) | 25.0 |
| Volume (L/hr) | 1.52448 |
| Fe(+3) Liq1 (mol/hr) | 0.104862 |
| H3OION Liq1 (mol/hr) | 0.106343 |
| pH | 1.2705 |

| strip adj. | |
|---|---|
| Volume (L/hr) | 1.5 |

| Solvent Recycle | |
|---|---|
| Volume Liq2 (L/hr) | 1.2496 |
| Fe(+3) Liq2 (mol/hr) | 5.03245e-3 |
| H2O Liq2, True (mol/hr) | 4.23443 |
| TBPHION Liq2 (mol/hr) | 9.09217e-3 |
| TRIBUTPHOS Liq2, True (mol/hr) | 4.27388 |

**Figure 11.** TBP stripping section of the calculated optimised ENICON017 (limonite) flowsheet.

This project has received funding from the European Union's EU
Framework Programme for Research and Innovation Horizon
Europe under Grant Agreement No 101058124
https://enicon-horizon.eu/

## 6.2 *Leaching: screening tests and optimisation of selected materials*

The materials studied in present project consists of ore material (laterites and sulphide concentrates), intermediates (FeNi, MHP, MSP) and tailings. The composition of these materials, both in terms of chemical composition as in terms of mineralogy, varies greatly. Table 1 below presents an overview of the chemical composition of the materials. For all of these materials, leaching conditions such as temperature, time, solid-over-liquid ratio (L/S, g $L^{-1}$) were optimised. For sulphidic materials and ferronickel, also $H_2O_2$ was added to aid the oxidation of the sulphides and metals (Fe, Ni, Co), respectively. While many experiments were performed on these materials, only the optimised conditions are shown in Table 2. While cobalt and nickel recoveries were high for most tested materials, only the carbonated tailings catch the eye due to their low leaching yields. Further, leaching of the sulphide concentrates require very low S/L ratios to obtain high recoveries for cobalt and nickel. Hence, the economic feasibility of such leaching process at current conditions is not feasible. Similarly, for the pyrite tailings, cobalt and nickel concentrations in the original material are too low for economic relevance. Hence, five materials can be selected for further optimisation: limonitic laterite ENICON017, saprolitic laterite ENICON028, ferronickel ENICON023, MHP ENICON013, MSP ENICON014. The leaching optimisation studies for the five selected materials will be discussed in more detail below.

**Table 1.** Chemical composition of the studied ENICON materials, in wt%.

| Sample type | Code | Co | Ni | Fe | Mn | Al | Mg | Ca | Si | Zn | Cu | Cr | S |
|---|---|---|---|---|---|---|---|---|---|---|---|---|---|
| **Laterite** | **016** | 0.03 | 0.92 | 14.62 | 0.24 | 0.40 | 7.90 | 5.08 | 16.42 | - | - | 0.45 | - |
| | **017** | 0.04 | 0.87 | 28.25 | 0.17 | 2.11 | 2.18 | 1.51 | 17.08 | - | - | 0.70 | - |
| | **020** | 0.05 | 0.88 | 38.16 | 0.37 | 2.09 | 1.55 | 2.86 | 11.99 | - | - | 1.12 | - |
| | **028** | 0.08 | 2.03 | 22.10 | 0.78 | 1.64 | 3.05 | 2.80 | 15.52 | - | | 0.66 | - |
| **FeNi** | **023** | 0.88 | 19.15 | 73.59 | - | - | 0.41 | 0.57 | 0.59 | - | - | - | - |
| | **024** | 0.59 | 23.94 | 76.40 | - | - | - | 0.05 | 0.31 | - | - | - | - |
| **MHP** | **011** | 25.75 | 15.42 | - | 1.06 | 0.90 | 0.33 | 0.12 | 1.04 | 0.30 | - | - | 4.6 |
| | **013** | 1.33 | 29.26 | 0.19 | 0.20 | 0.03 | 0.95 | 0.08 | | 0.61 | 0.03 | | 10.6 |
| **MSP** | **012** | 40.02 | 20.19 | 0.37 | - | 0.22 | 0.07 | 0.11 | 0.85 | 0.22 | - | - | 25.7 |
| | **014** | 1.87 | 44.41 | 0.77 | - | 0.04 | 0.09 | - | - | 0.79 | - | - | 26.3 |
| **Ni/Co concentrate** | **002B** | 0.51 | 9.39 | 40.46 | 0.03 | 0.28 | 3.58 | 1.30 | 6.88 | - | 1.61 | 0.04 | nd* |
| | **003** | 1.63 | 6.77 | 42.31 | 0.02 | 0.35 | 2.50 | 0.79 | 7.38 | 0.02 | 0.01 | 0.20 | 26 |
| **Pyrite tailings** | **004** | 0.05 | 1.08 | 35.11 | 0.07 | 0.86 | 7.9 | 0.84 | 12.33 | - | 0.21 | 0.12 | 16 |
| | **007** | 0.05 | 0.04 | 7.53 | 0.05 | 0.97 | 2.30 | 1.31 | 28.58 | - | - | 0.03 | nd* |
| **Carbonated Clinkers** | | **0.01** | 0.07 | 5.57 | 0.1 | 1.58 | 9.07 | 16.48 | 17.3 | - | 0.05 | 0.17 | - |

*nd = not determined

**Table 2**. Optimised leaching conditions during bench-scale screening tests for the ENICON materials.

| | | Leaching conditions | | | | | Recovery (%) | |
|---|---|---|---|---|---|---|---|---|
| **Material** | **Code** | **HCl (M)** | **$H_2O_2$ (vol.% )** | **S/L ($g\ L^{-1}$)** | **Temp. (°C)** | **Time (h)** | **Co** | **Ni** |
| **Laterite (Saprolitic)** | 016 | 8 | - | 200 | 95 | 3 | 86 | 99 |
| **Laterite (Limonitic)** | 017 | 8 | - | 200 | 80 | 3 | 89 | 95 |
| **Laterite (Saprolitic)** | 020 | 8 | - | 100 | 95 | 3 | 97 | 100 |
| **Laterite (Saprolitic)** | 028 | 8 | - | 200 | 80 | 3 | 94 | 95 |
| **FeNi** | 023 | 8 | 5 | 100 | 95 | 2 | 100 | 100 |
| | 024 | 5 | 5 | 40 | 95 | 2 | 100 | 100 |
| **MHP** | 011 | 4 | - | 200 | 80 | 3 | 95 | 97 |
| | 013 | 4 | - | 200 | 25 | 2 | 98 | 99 |
| **MSP** | 012 | 8 | 10 | 20 | 95 | 3 | 100 | 100 |
| | 014 | 8 | 10 | 50 | 60 | 8 | 90 | 97 |
| **Ni/Co concentrate** | 002B | 8 | 10 | 40 | 90 | 3 | 92 | 94 |
| | 003 | 8 | 10 | 25 | 90 | 3 | 93 | 95 |
| **Pyrite tailings** | 004 | 8 | 10 | 40 | 95 | 3 | 99 | 94 |
| | 007 | 8 | 8 | 100 | 95 | 3 | 96 | 99 |
| **Carbonated clinkers** | no code | 8 | 0 | 100 | 60 | 2 | 47 | 58 |

### *6.2.1 Ferronickel (FeNi)*

The leaching of the FeNi was performed without prior crushing of the material, as none of the available mills or shredders were able to reduce the size of the FeNi pellets. Nevertheless, leaching of these materials was very efficient. Both ENICON023 and ENICON024 materials were very similar in terms of composition and reactivity, hence it was opted to optimise the leaching (and solvent extraction) process for one of the materials (ENICON023), as results would have been identical with the other material. Using the optimised parameters, as indicated in Table 2, quantitative leaching of nickel and cobalt was obtained within 3 hours (Figure 12). The ORP remained relatively stable (+400 mV vs. Ag/AgCl) throughout the leaching test due to the gradual addition of 90 mL of a 30 wt% $H_2O_2$ solution over this time period. This also prevented most of the $H_2$ formation during leaching. Table 3 shows the final composition of the PLS after the 8-hour leaching test.

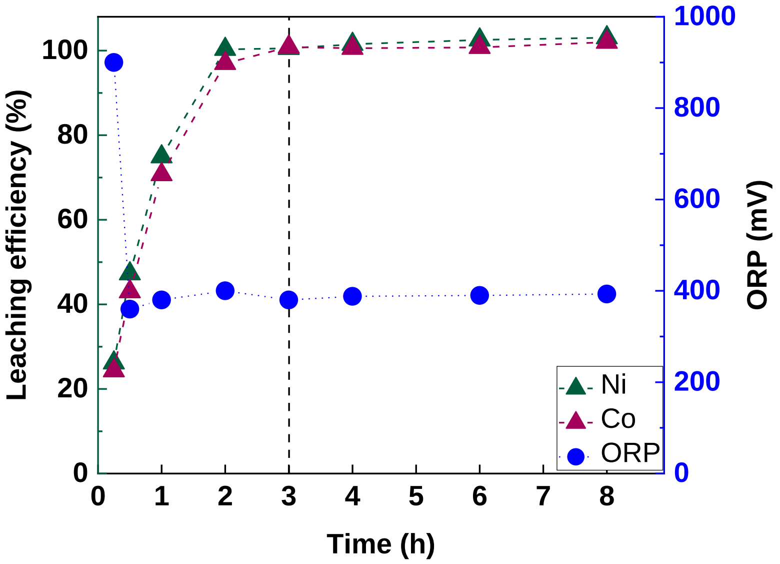

**Figure 12.** Leaching kinetics of nickel and cobalt for FeNi ENICON023. Conditions: 8 mol L$^{-1}$ HCl, 10 vol% of a 30 wt% $H_2O_2$ solution, S/L = 100 g L$^{-1}$, 8 hours, 60 °C, 110 rpm, total volume 900 mL. ORP in mV vs. Ag/AgCl.

**Table 3.** PLS composition and HCl consumption after FeNi (ENICON023) leaching on 900 mL scale. Conditions: 8 mol L$^{-1}$ HCl, 10 vol% of a 30 wt% $H_2O_2$ solution, S/L = 100 g L$^{-1}$, 8 hours, 60 °C, 110 rpm.

| g L$^{-1}$ | | | | | mol L$^{-1}$ | kg HCl / kg FeNi |
|---|---|---|---|---|---|---|
| **Co** | **Ni** | **Fe** | **Mg** | **Ca** | **Free HCl** | **HCl consumption** |
| 0.9 | 20.1 | 72.4 | 0.02 | 0.02 | 1.8 | 1.9 |

### 6.2.2 *Limonite and saprolite*

Screening tests to optimise leaching conditions were performed on the crushed material with an average particle size of ≤500 µm. However, for the scale-up leaching tests, no prior treatment was applied. All four laterite materials have very similar metal compositions and chemical behaviour, leading to the selection of one limonite (ENICON 017) and one saprolite (ENICON 028) sample, both containing significant concentrations of the target metals, Ni and Co. Using identical leaching parameters (Table 2) for both materials on a larger scale (900 mL), high cobalt and nickel recoveries were obtained within limited time range (Figure 13–14). Leaching kinetics for the limonite were slightly slower, with just above 80% recovery of nickel and cobalt after 3 hours, while for the saprolite leaching experiment, recoveries of around 95% were measured for both elements. Eventually, after 8 hours, 95% of nickel and 89% of cobalt was recovered from the limonite. The ORP slightly decreased throughout the experiment, yet remained higher than +600 mV (vs. Ag/AgCl), which is typical for concentrated Fe(III) solutions. Table 4 shows the final composition of the PLS after the 8-hour leaching test.

This project has received funding from the European Union's EU Framework Programme for Research and Innovation Horizon Europe under Grant Agreement No 101058124
https://enicon-horizon.eu/

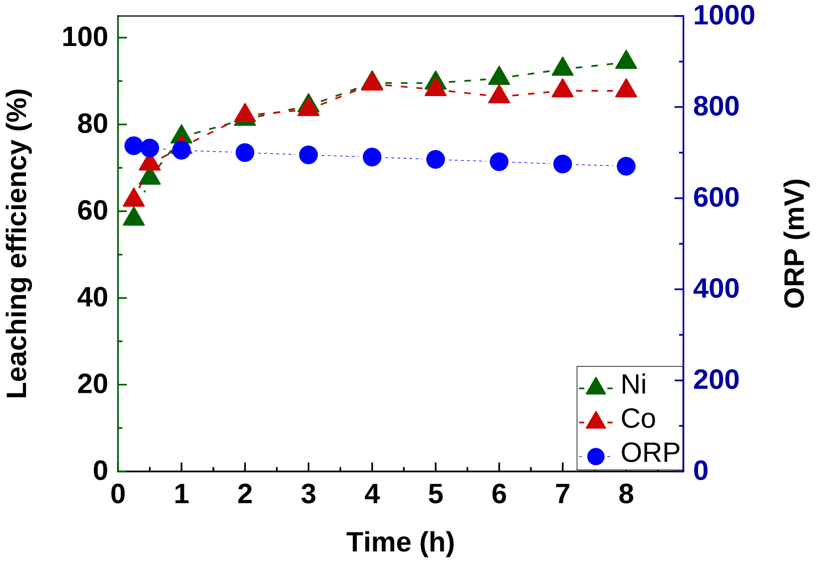

**Figure 13.** Leaching kinetics of nickel and cobalt for limonite ENICON017. Conditions: 8 mol L$^{-1}$ HCl, S/L = 200 g L$^{-1}$, 8 hours, 80 °C, 200 rpm, total volume 900 mL. ORP in mV vs. Ag/AgCl.

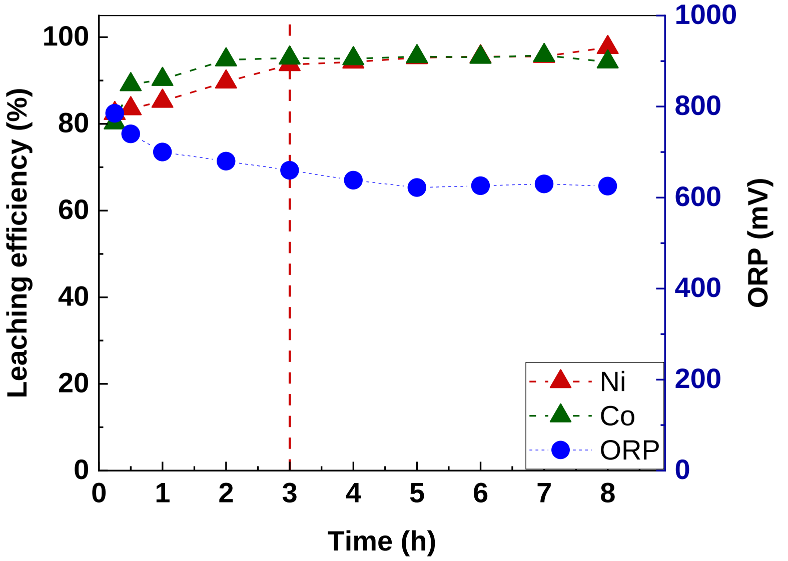

**Figure 14.** Leaching kinetics of nickel and cobalt for saprolite ENICON028. Conditions: 8 mol L$^{-1}$ HCl, S/L = 200 g L$^{-1}$, 8 hours, 80 °C, 200 rpm, total volume 900 mL. ORP in mV vs. Ag/AgCl.

This project has received funding from the European Union's EU
Framework Programme for Research and Innovation Horizon
Europe under Grant Agreement No 101058124
https://enicon-horizon.eu/

**Table 4.** PLS composition and HCl consumption after limonite (ENICON017) and saprolite (ENICON028) leaching on 900 mL scale. Conditions: 8 mol $L^{-1}$ HCl, S/L = 200 g $L^{-1}$, 8 hours, 80 °C, 200 rpm.

| | **g $L^{-1}$** | | | | | | | | **mol $L^{-1}$** | **kg HCl/ kg laterite** |
|---|---|---|---|---|---|---|---|---|---|---|
| **Laterite Type** | **Co** | **Ni** | **Fe** | **Mg** | **Al** | **Ca** | **Mn** | **Cr** | **Free HCl** | **HCl consumption** |
| **Limonite** | 0.1 | 1.6 | 57.2 | 4.6 | 3.9 | 2.6 | 0.3 | 0.8 | 2.3 | 0.9 |
| **Saprolite** | 0.2 | 4.3 | 45.3 | 7.5 | 3.1 | 5.2 | 1.5 | 0.7 | 3.6 | 0.7 |

### *6.2.3 MHP and MSP*

A set of leaching tests was performed without prior pre-treatment on both MHP samples, ENICON 011 and ENICON 013. Almost complete extraction of Ni and Co was obtained for both materials with similar behaviour. However, due to the limited amount of ENICON 011, ENICON 013 was selected for further optimisation of the leaching and solvent extraction process at the bench and scale-up levels. Using the optimised parameters, as indicated in Table 2, quantitative leaching of nickel and cobalt, i.e. 99% and 98%, respectively, was obtained within the first hour (Figure 15). The ORP remained stable throughout the experiment at +1000 mV (vs. Ag/AgCl). Table 5 shows the final composition of the PLS. Note that there is a significant amount of sulphate present in this PLS. The MHP ENICON013 was not washed after the precipitation during its production, and hence, large amounts of $Na_2SO_4$ are still present (Table 6). The amount of S present as sulphide is limited. Hence, the leaching of MHP, ENICON 013, was later evaluated after water pre-treatment (S/L = 100 g/L, 1 h, RT, 400 RPM) to remove $Na_2SO_4$ from the sample. A proof-of-principle leaching test on the washed MHP showed that similar metal recoveries were only obtained at lower S/L ratios. While only around 50% of cobalt and nickel were leached at 400 g $L^{-1}$ using 4 mol $L^{-1}$ HCl, almost 100% of both metals were recovered at 200 g $L^{-1}$ using the same lixiviant. All other parameters were identical to the test shown in Figure 15. These results make sense, as the washed MHP now has much higher cobalt and nickel concentrations, i.e. 2.3 wt% and 47.7 wt%, respectively, compared to the unwashed material. The MHP lost about 40% of its original weight after washing.

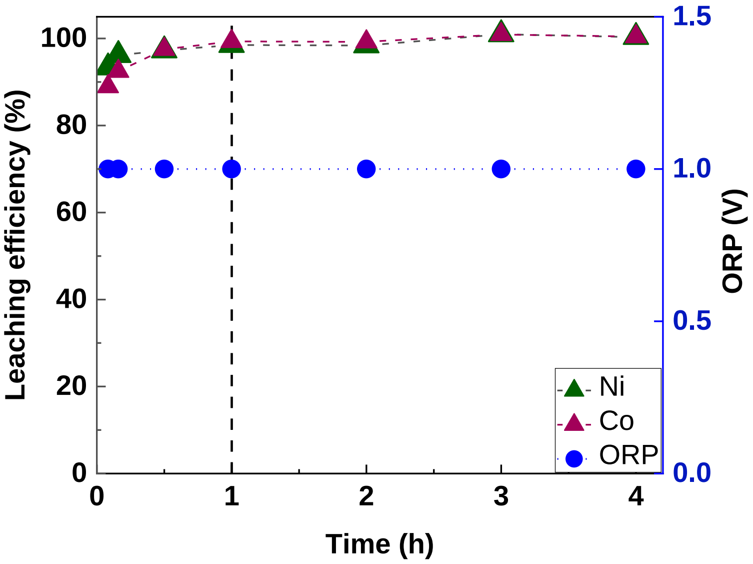

**Figure 15.** Leaching kinetics of nickel and cobalt for unwashed MHP ENICON013. Conditions: 4 mol $L^{-1}$ HCl, S/L = 360 g $L^{-1}$, 4 hours, 21 °C, 150 rpm, total volume 900 mL. ORP in mV vs. Ag/AgCl.

**Table 5.** PLS composition and HCl consumption after unwashed MHP (ENICON013) leaching on 900 mL scale. Conditions: 4 mol $L^{-1}$ HCl, S/L = 360 g $L^{-1}$, 4 hours, 21 °C, 150 rpm.

| g $L^{-1}$ | | | | | | | | mol $L^{-1}$ | kg HCl/ kg MHP |
|---|---|---|---|---|---|---|---|---|---|
| **Co** | **Ni** | **Fe** | **Mg** | **Zn** | **Ca** | **Mn** | **$SO_4^{2-}$** | **Free HCl** | **HCl consumption** |
| 4.9 | 103.2 | 0.6 | 3.2 | 1.2 | 0.5 | 0.5 | 115 | ≤0.01 | 0.4 |

**Table 6.** Sulphur content in unwashed and washed MHP (ENICON013).

| Sample | Total S (wt%) |
|---|---|
| **Unwashed MHP** | 10.6 |
| **Washed MHP** | 3.2 |

This project has received funding from the European Union's EU
Framework Programme for Research and Innovation Horizon
Europe under Grant Agreement No 101058124
https://enicon-horizon.eu/

Leaching tests were conducted on both MSP samples, ENICON 012 and ENICON 014, without any pre-treatment. Both materials showed similar behaviour, achieving nearly complete extraction of Ni and Co. ENICON 014 was chosen for further refinement of the leaching and solvent extraction processes at both bench and scale-up stages. While the metal composition in MHP and MSP are similar, different precautions and leaching conditions needed to be chosen due to the presence of the metals as sulphides instead of hydroxides. In all leaching conditions, the addition of $H_2O_2$ was necessary to improve leaching efficiency and ensure safety by inhibiting $H_2S$ formation. Moreover, the S/L ratio seemed to play a significant role, and high leaching yields were obtained only at low S/L ratios. Using the optimised parameters, as indicated in Table 2, about 90% of cobalt and 97% of nickel were recovered (Figure 16). Minor amount of a black residue was left after leaching, presumably elemental sulphur, with some of the non-leached metals. As Table 7 presents the composition of the PLS after the 8-hour leaching experiment. While, based on theoretical calculations, about 17 g $L^{-1}$ sulphate was expected, about 20 g $L^{-1}$ was measured using ion chromatography. This amount of sulphates might complicate the chloride-based process to be developed within ENICON, yet sulphates could either be removed through precipitation (e.g. calcium) or could be avoided by working at less oxidizing conditions during leaching, i.e. lower ORP values. ORP values were indeed high (> +800 mV, vs. Ag/AgCl) during the initial hours of the leaching experiment, and decreased gradually to about +500 mV (vs. Ag/AgCl).

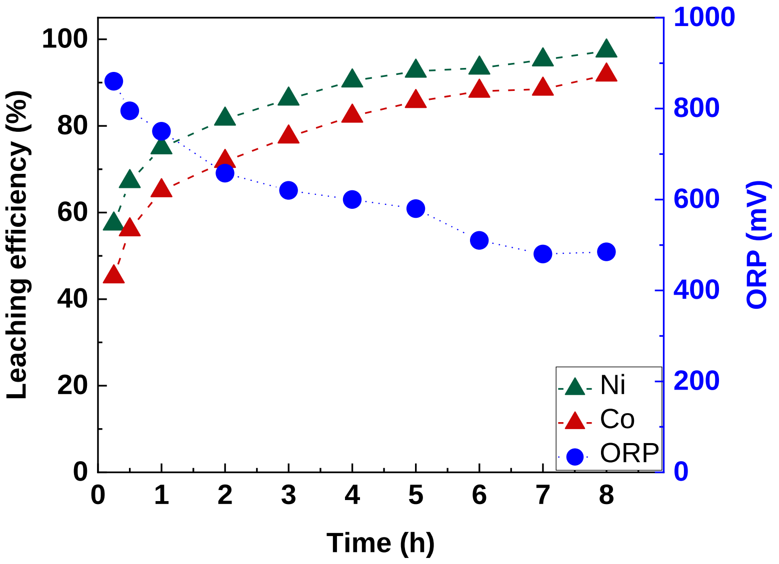

**Figure 16.** Leaching kinetics of nickel and cobalt for MSP ENICON014. Conditions: 8 mol $L^{-1}$ HCl, 10 vol% of 30 wt% $H_2O_2$ solution, S/L = 50 g $L^{-1}$, 8 hours, 60 °C, 200 rpm, total volume 900 mL. ORP in mV vs. Ag/AgCl.

**Table 7.** PLS composition and HCl consumption after MSP (ENICON014) leaching on 900 mL scale. Conditions: 8 mol $L^{-1}$ HCl, 10 vol% of 30 wt% $H_2O_2$ solution, S/L = 50 g $L^{-1}$, 8 hours, 60 °C, 200 rpm.

| g $L^{-1}$ | | | | | | mol $L^{-1}$ | kg HCl/ kg MSP |
|---|---|---|---|---|---|---|---|
| **Co** | **Ni** | **Fe** | **Mg** | **Zn** | **$SO_4^{2-}$** | **Free HCl** | **HCl consumption** |
| 0.9 | 22.1 | 0.4 | 0.04 | 0.3 | 20 | 4.2 | 0.9 |

This project has received funding from the European Union's EU Framework Programme for Research and Innovation Horizon Europe under Grant Agreement No 101058124
https://enicon-horizon.eu/

## 6.3 Solvent extraction

### 6.3.1 Ferronickel (FeNi)

The main objective in the case of the FeNi PLS is the removal of Fe(III) and excess HCl by solvent extraction. Hence, TBP is used as the extractant, in order to remove all $FeCl_3$ and most HCl from the aqueous phase. The extraction reaction shown below (Equation 5) indicates that Fe(III) is extracted together with an equimolar amount of HCl, with the overbar signifying species in the organic phase. Hence, the leaching of FeNi as describe above was slightly adjusted to have almost equimolar amounts of Fe(III) and HCl in the PLS, with slightly more HCl than Fe(III) to keep all elements in solution. The resulting PLS is shown below in Table 8, with 1.5 mol $L^{-1}$ Fe(III) and 1.7 mol $L^{-1}$ HCl. After leaching, iron occurs as Fe(II) in the PLS. To be efficiently extracted, Fe(II) has to undergo oxidation to Fe(III). Hence, three different approaches were tested: oxidation by air, by oxygen gas and by $H_2O_2$. The oxidation kinetics by air and oxygen gas appeared to be very slow (Figure 17–18). The oxidation of Fe(II) by $O_2$, be it in air or as a pure gas, proceeds via the thermodynamical unfavourable formation of an oxygen radical, which is the rate-limiting step during oxidation. Besides, increasing temperature has an obviously positive effect on the oxidation rate. At 60 °C, about 80% of Fe(II) was oxidised after 180 h when using compressed air, while almost quantitative oxidation was observed after 24 h when using $O_2$ gas. At room temperature, the percentage Fe(III) versus total iron content was only about 40% and 55% for compressed air and $O_2$ gas, respectively. The third approach, using $H_2O_2$ as an oxidiser, was more efficient and industrially more relevant, seen the short residence time and low temperature (room temperature). Figure 19 shows that a slight excess of $H_2O_2$, i.e. 25% above the theoretical stoichiometry, is necessary to fully oxidise Fe(II). The oxidation reaction occurs practically instantaneously, although care should be taken as the reaction mixture heats up and starts to foam slightly upon addition of the $H_2O_2$. Hence, slow addition of $H_2O_2$ is advised.

$$FeCl_3 + HCl + \overline{TBP} \rightleftarrows \overline{[FeCl_4^-][TBPH^+]} \tag{5}$$

**Table 8.** Composition of the FeNi (ENICON 023) PLS prior to oxidation.

| g $L^{-1}$ | | | | | | | mol $L^{-1}$ |
|---|---|---|---|---|---|---|---|
| **Co** | **Ni** | **Fe** | **Mg** | **Ca** | **Zn** | **Cu** | **HCl** |
| 1.0 | 21.7 | 84.2 | 19 | 36 | 135 | 65 | 1.7 |

This project has received funding from the European Union's EU Framework Programme for Research and Innovation Horizon Europe under Grant Agreement No 101058124
https://enicon-horizon.eu/

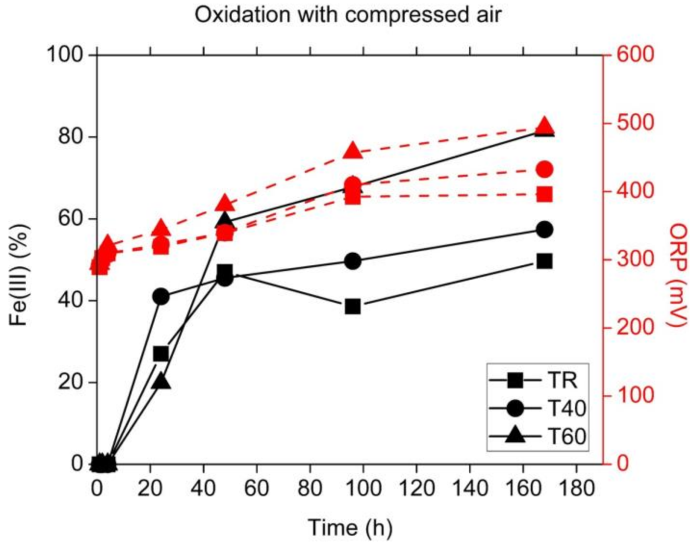

**Figure 17.** Oxidation of Fe(II) to Fe(III) by compressed air. Conditions: [Fe] = 75.7 g $L^{-1}$; initial ORP +290 mV (vs. Ag/AgCl)

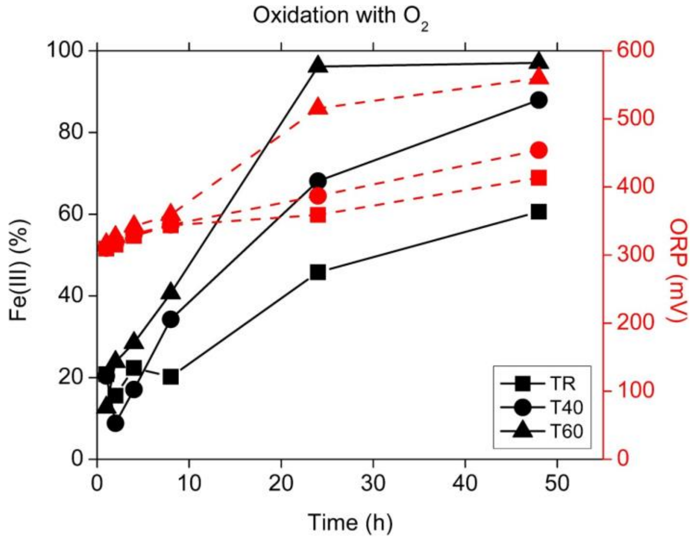

**Figure 18.** Oxidation of Fe(II) to Fe(III) by oxygen gas. Conditions: [Fe] = 75.7 g $L^{-1}$; initial ORP +300 mV (vs. Ag/AgCl).

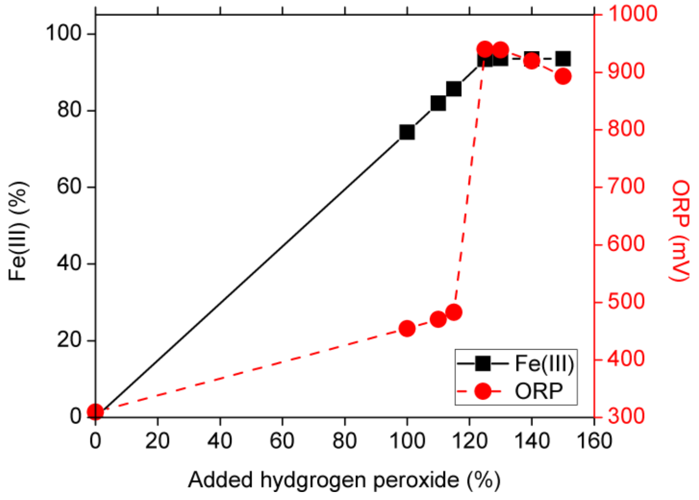

**Figure 19.** Amount of hydrogen peroxide (30 wt%) added, where 100% equals the stoichiometric amount. Conditions: [Fe] = 73.7 g $L^{-1}$; [HCl] = 2.46 mol/L; initial ORP +310 mV (vs. Ag/AgCl).

Once a fully oxidised PLS is obtained, extraction by undiluted, water-presaturated TBP is performed. Figure 20 shows a McCabe-Thiele diagram constructed using the distribution isotherm of Fe(III). This indicates that, theoretically, 2 or 3 counter-current stages would be needed to lower Fe(III) concentration to about 16 g L-1, at O:A = 2:1 or 3:2, respectively. An additional 1 or 2 stages would be needed for quantitative removal of Fe(III). To verify this, a counter-current extraction simulation (CCES) was performed, simulating 5 counter-current stages at O:A = 3:2. Figure 21 indeed shows that about 97% of Fe(III) and 94% of HCl were extracted using these conditions, which means that only 2.08 g $L^{-1}$ Fe(III) and 0.1 mol $L^{-1}$ free HCl are left in the raffinate. Although most of the acid has thus been recovered, downstream use of this raffinate might still require the addition of base to raise pH to attain optimal conditions. Regarding the purity of nickel, if a MHP were to be made from the current raffinate, the concentration of nickel in this MHP would exceed 50 wt%, which is more than the key performance indicator (KPI) of 42 wt% envisioned in the ENICON project.

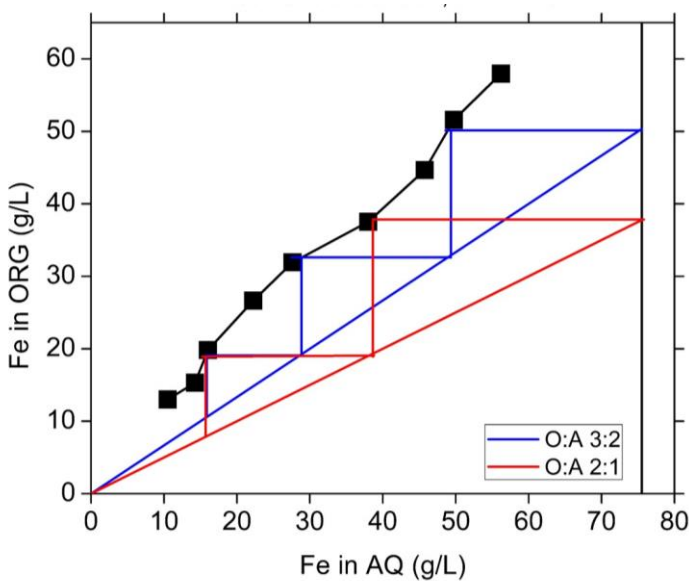

**Figure 20**. McCabe-Thiele diagram for Fe(III) extraction by undiluted TBP. Conditions: $[Fe]_A$ = 78.3 g $L^{-1}$; $[HCl]_A$ = 1.7 mol $L^{-1}$; 500 rpm, 1h, room temperature.

This project has received funding from the European Union's EU
Framework Programme for Research and Innovation Horizon
Europe under Grant Agreement No 101058124
https://enicon-horizon.eu/

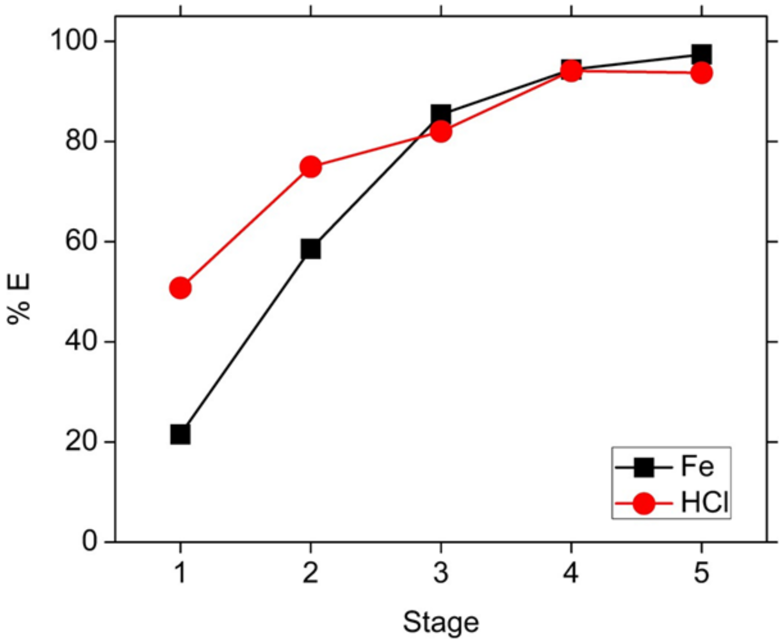

**Figure 21.** Five–stage CCES of PLS with undiluted, water–presaturated TBP. Conditions: $[Fe]_A$ = 78.3 g $L^{-1}$; $[HCl]_A$ = 1.7 mol $L^{-1}$; O:A = 3:2 (15 mL : 10 mL); 15 minutes; 300 rpm; room temperature.

Next, the loaded organic obtained after 5-stage counter-current extraction is contacted with water at room temperature, to strip the extracted $FeCl_3$ and HCl. The effect of the O:A phase ratio, as presented in Figure 22, indicates that the stripping efficiencies for HCl and Fe(III) overlap, which is expected from Equation 5. A McCabe-Thiele diagram for stripping of Fe(III) based on these results is presented in Figure 23 and shows that about 4 stages would be necessary to remove all Fe(III) at O:A = 2:3. Likewise, HCl is likely to be stripped quantitatively, seen the extraction reaction and results presented above. Hence, an aqueous strip raffinate containing approximately 46 g $L^{-1}$ Fe(III) and 0.7 mol $L^{-1}$ HCl is obtained. This is to be further processed through hydrolytic distillation (*vide infra*), to recover all HCl and transform $FeCl_3$ into hematite ($Fe_2O_3$).

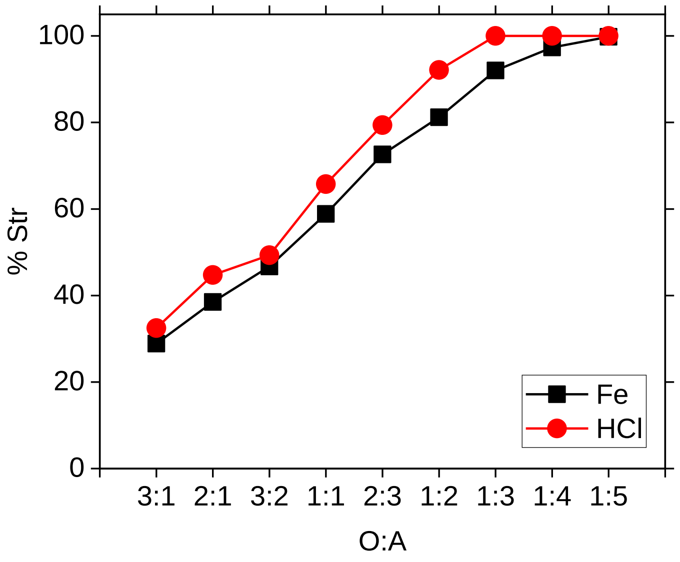

**Figure 22.** Effect of the phase ratio on Fe(III) and HCl stripping from loaded TBP with water. Conditions: $[Fe]_O$ = 68.3 g $L^{-1}$; $[HCl]_O$ = 1.07 mol $L^{-1}$; 500 rpm, 1h, room temperature.

This project has received funding from the European Union's EU
Framework Programme for Research and Innovation Horizon
Europe under Grant Agreement No 101058124
https://enicon-horizon.eu/

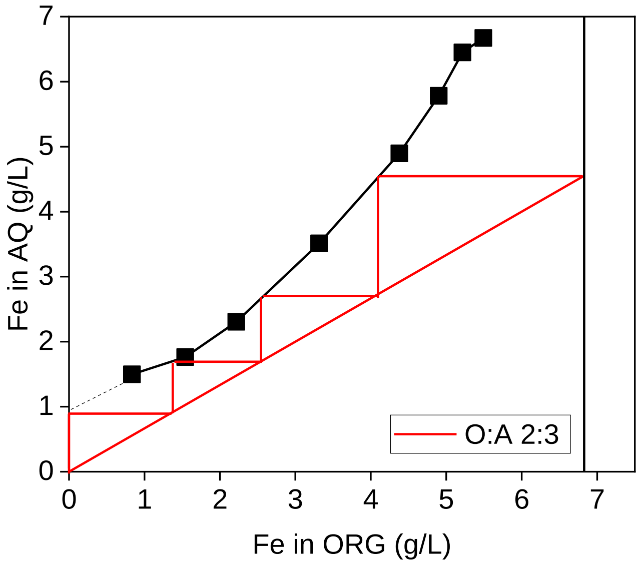

**Figure 23**. McCabe-Thiele diagram for Fe(III) stripping from undiluted TBP by water. Conditions: $[Fe]_O$ = 68.3 g $L^{-1}$; $[HCl]_O$ = 1.07 mol $L^{-1}$; 500 rpm, 1h, room temperature.

Eventually, the flowsheet presented in Figure 24 can be proposed for the processing of FeNi to obtain battery-grade nickel (and cobalt), based on above optimisation studies. The solvent extraction conditions are to be tested in continuous counter-current mixer settlers (*Deliverable 2.5 Final report on the pilot-level demonstration of next-generation HCl-route, M46*). The purified raffinate, containing only Co(II) Ni(II), and residual HCl (< 0.7 mol $L^{-1}$) can be further treated by the processes developed in WP3, i.e. *Task 3.1 Development of Ni/Co ultra-refining process through Direct Oxide Recovery* and *Task 3.2 Ultra-refining of Ni/Co-intermediate from next-gen' HCl-route in an existing hydro-process*.

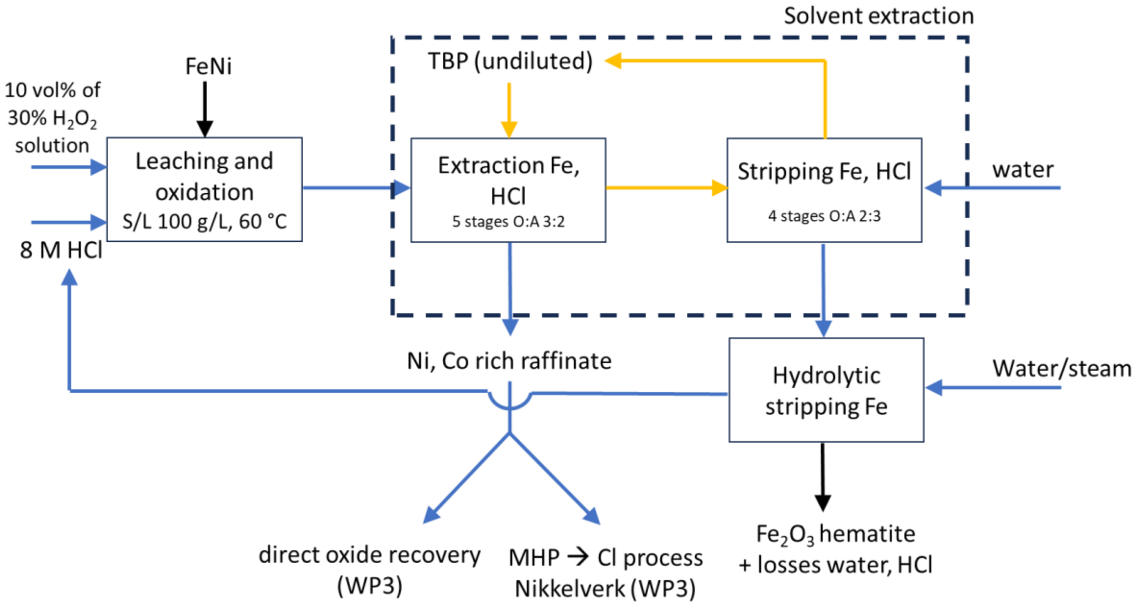

**Figure 24.** Preliminary flowsheet for the upgrading of ferronickel (FeNi) to battery-grade nickel (and cobalt) using the ENICON HCl-based process.

This project has received funding from the European Union's EU Framework Programme for Research and Innovation Horizon Europe under Grant Agreement No 101058124
https://enicon-horizon.eu/

### 6.3.2 *Saprolite and limonite*

Laterites can be divided into saprolitic laterites, which are richer in magnesium and have a slightly higher nickel concentration, and limonitic laterites, which contain less magnesium and nickel, but have a higher iron content.[2] These usually occur together in laterite deposits, with limonite forming the upper layer of the deposit, and the saprolite the lower layer. These two types are usually processed in a slightly different manner, i.e. limonitic laterites are usually treated by the HPAL-method (vide supra), while saprolitic laterites are processed via smelting. In the ENICON project, both are studied as the HCl process could prove to be a greener alternative for the recovery of cobalt and nickel from these resources. Specifically, the limonite ENICON017 and the saprolite ENICON028 were studied. The PLS obtained using the optimised leaching conditions (*vide supra*) has a composition as presented in Table 9. As is obvious from the above statement, the saprolite PLS is richer in nickel and magnesium, while the limonite PLS is richer in iron. For both laterite types, the Fe(III) concentration is sufficiently high to co-extract Fe(III) together with HCl using TBP, as has been proven to work efficiently for the FeNi PLS. For the development of the flowsheet, it was chosen to optimise the solvent extraction parameters for the saprolite sample, as its composition is slightly more challenging seen the higher concentration of Mg(II), Ca(II) and Mn(II), yet the value is slightly higher due to the higher Ni(II) concentration. Eventually the optimised parameters will be tested out on the limonitic saprolite, when before scaling-up the solvent extraction process on mixer-setters (*Deliverable 2.5 Final report on the pilot-level demonstration of next-generation HCl-route, M46*).

Before starting with the removal of Fe(III) by TBP, it is important to check the results of the modelling (*vide supra*). Ideally, there should be an equimolar amount of Fe(III) and free HCl in solution, to attain optimal recovery of both. The PLS produced by the conditions that were optimal for leaching, however, there was 3 times the number of moles of HCl compared to Fe(III), and hence, recovery of HCl would not be optimal. This can also be seen from Figure 25, investigating the influence of the phase ration on the extraction of metals from the PLS produced using the original leaching conditions. Only a third of HCl was extracted at the highest O:A ratio, while all Fe(III) was extracted. Hence, it was opted to revise the leaching conditions: the S/L ratio increased from 200 to 300 g L$^{-1}$ and the initial HCl concentration in the lixiviant decreased from 8 to 6 mol L$^{-1}$. While this decreased leaching efficiency (Ni: 96% to 87%, Co: 96% to 83%, Fe: 95% to 66%), the molar ratio of HCl to Fe(III) decreased significantly.

**Table 9.** Composition of the limonitic (ENICON017) and saprolitic (ENICON028) laterite PLS. Leaching conditions: (A) 8 mol L$^{-1}$ HCl, S/L = 200 g L$^{-1}$, 8 hours, 80 °C, 200 rpm; (B) 6 mol L$^{-1}$ HCl, S/L = 300 g L$^{-1}$, 5 hours, 90 °C, 200 rpm.

| | | **g L$^{-1}$** | | | | | | | | **mol L$^{-1}$** |
|---|---|---|---|---|---|---|---|---|---|---|
| **Laterite type** | **leaching conditions** | **Co** | **Ni** | **Fe** | **Mg** | **Al** | **Ca** | **Mn** | **Cr** | **HCl** |
| **Limonite** | A | 0.1 | 1.6 | 57.2 | 4.6 | 3.9 | 2.6 | 0.3 | 0.8 | 2.3 |
| **Saprolite** | A | 0.2 | 4.3 | 45.3 | 7.5 | 3.1 | 5.2 | 1.5 | 0.7 | 3.6 |
| | B | 0.2 | 5.1 | 46.5 | 9.0 | 2.6 | 6.3 | 2.0 | 0.6 | 1.6 |

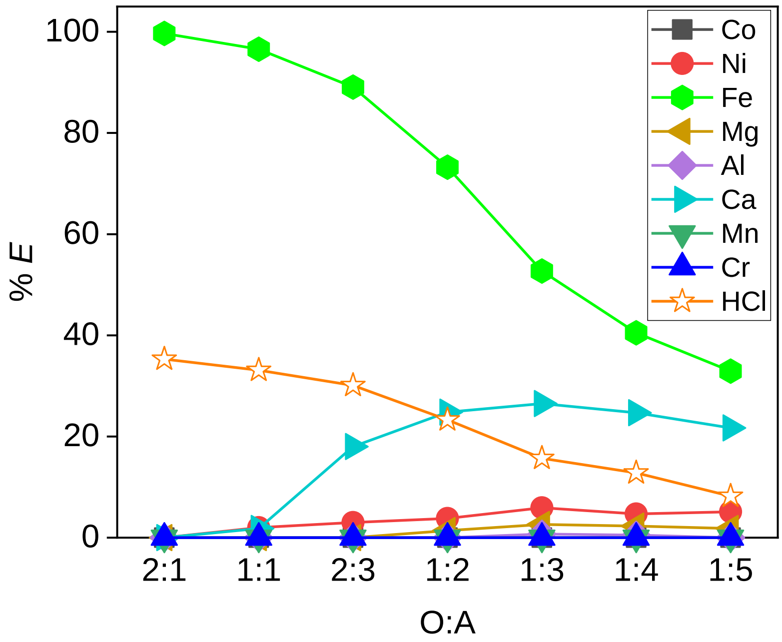

**Figure 25.** Effect of the organic-to-aqueous phase ratio on Fe(III) and HCl extraction by water-presaturated, undiluted TBP. Conditions: $[Fe]_A$ = 45.3 g $L^{-1}$; $[HCl]_A$ = 3.6 mol $L^{-1}$; 500 rpm, 1h, room temperature.

Eventually, a McCabe-Thiele diagram based on the extraction isotherm for Fe(III) and HCl was constructed, as shown in Figure 26 –27. It can be seen that complete extraction of HCl might be challenging, as even at high O:A ratios, many stages would be needed, while Fe(III) can be readily extracted at O:A = 5:4. This makes sense, as there is still a slight excess of HCl present in the new PLS, and once all Fe(III) is extracted, only of the remaining free HCl is taken up by TBP. Therefore, it was attempted to remove all Fe(III) in 2 cross-current contacts of the PLS with fresh, undiluted TBP. This resulted in a raffinate that contained only 62 mg $L^{-1}$ Fe(III), yet still had 0.52 mol $L^{-1}$ free HCl (pH 0.28). In order to continue, two routes were studied: (1) partial neutralisation with base (NaOH) to pH 5.5, prior to solvent extraction with Versatic Acid 10, (2) increasing pH to about 3 – 4 by using TEHA to extract excess HCl, prior to solvent extraction with Versatic Acid 10. The partial neutralisation leads to the precipitation of chromium, aluminium, iron and losses of nickel (20%) and cobalt (30%) due to co-precipitation. These losses could be avoided when using TEHA to extract excess HCl. The McCabe-Thiele diagram for HCl extraction by TEHA is shown in Figure 28, and indicates that 2 to 3 counter-current stages would be needed for almost complete removal of HCl at O:A = 3:1 or 2:1, respectively. Using the same organic phase, 4 cross-current contacts at O:A = 3:1 was able to remove most of the HCl, with pH values reaching 3.2 (Figure 29), without losses of metals in the aqueous phase. The raffinate thus produced was then contacted with a 20 vol% Versatic Acid 10, diluted in Shellsol D70, and pH was adjusted accordingly to construct the pH isotherms for the metals in the solution. However, around pH 4 – 4.5, a precipitate began to form in the solvent extraction samples, probably due to hydrolysis of aluminium and chromium (Figure 30). It is therefore advised to either remove these elements prior to this solvent extraction step, or to saponify the extractant, for instant by using MgO. Finally, a flowsheet as shown in Figure 31 could be presented, where the process steps marked in green are those already studied and/or optimised, and the white steps have still to be investigated. It can be proposed to strip the Versatic Acid 10, loaded with cobalt, nickel and manganese, with sulphuric acid instead, to enhance the separation between manganese and the other two metals when doing a precipitation step using ammonia/ammonium carbonate. An identical flowsheet for the limonite would work equally well, although the leaching parameters would also need to be adjusted to obtain near-equimolar amounts of Fe(III) and HCl in the laterite PLS. Eventually, the Ni/Co sulphate solution is to be further purified in WP3, WP3, i.e. *Task 3.1 Development of Ni/Co ultra-refining process through Direct Oxide Recovery* and *Task 3.2 Ultra-refining of Ni/Co-intermediate from next-gen' HCl-route in an existing hydro-process*.

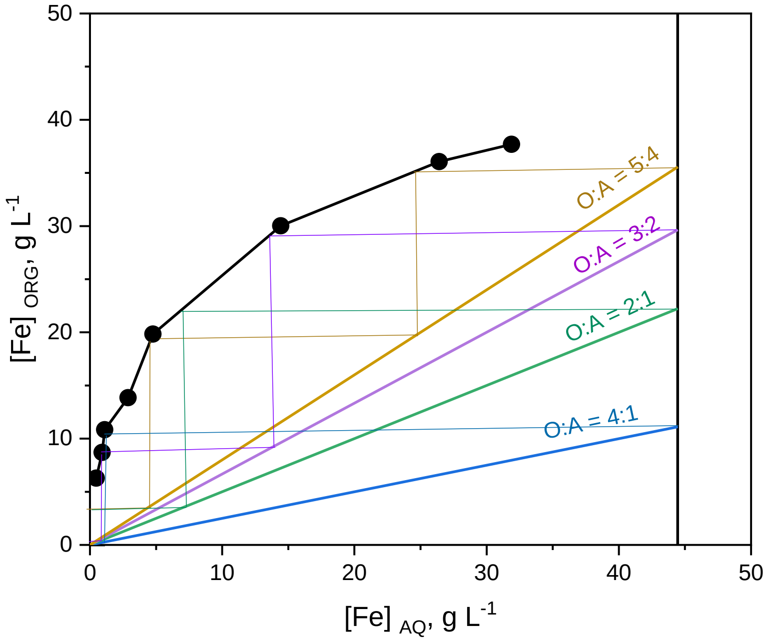

**Figure 26.** McCabe-Thiele diagram for Fe(III) extraction by undiluted TBP. Conditions: $[Fe]_A$ = 46.5 g $L^{-1}$; $[HCl]_A$ = 1.6 mol $L^{-1}$; 500 rpm, 1h, room temperature.

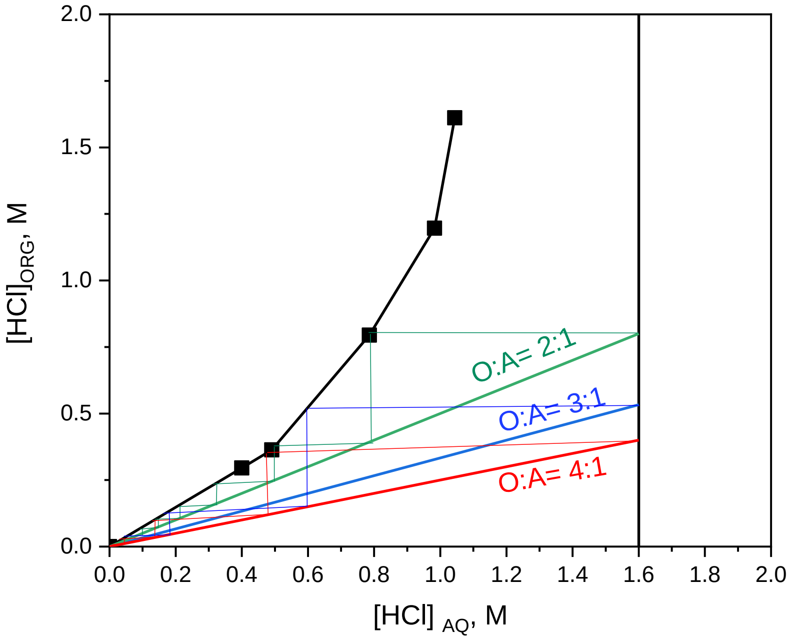

**Figure 27.** McCabe-Thiele diagram for HCl extraction by undiluted TBP. Conditions: $[Fe]_A$ = 46.5 g $L^{-1}$; $[HCl]_A$ = 1.6 mol $L^{-1}$; 500 rpm, 1h, room temperature.

This project has received funding from the European Union's EU
Framework Programme for Research and Innovation Horizon
Europe under Grant Agreement No 101058124
https://enicon-horizon.eu/

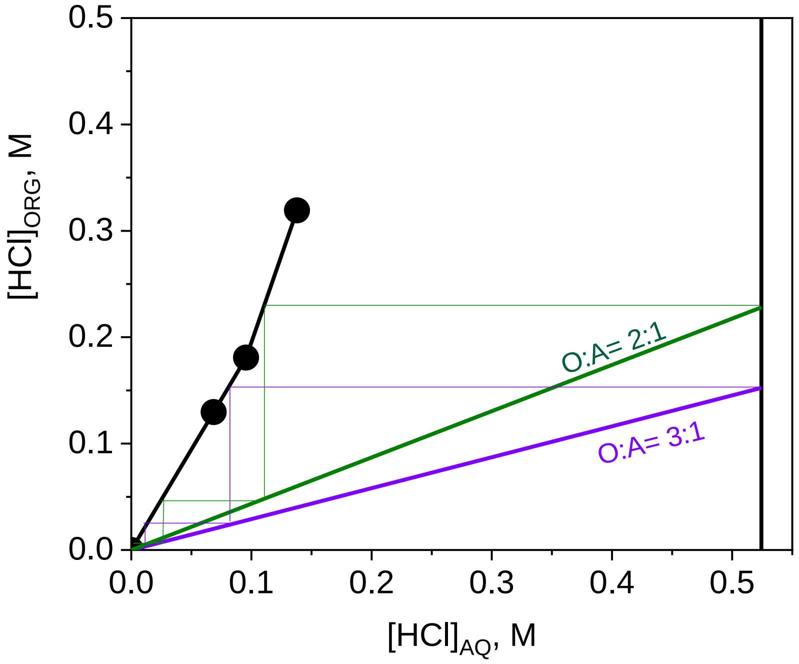

**Figure 28.** McCabe-Thiele diagram for HCl extraction by 50 vol% TEHA. Conditions: $[HCl]_A$ = 0.52 mol $L^{-1}$, organic phase: 50 vol% TEHA + 5 vol% 1-decanol in D70 diluent, 500 rpm, 1h, room temperature.

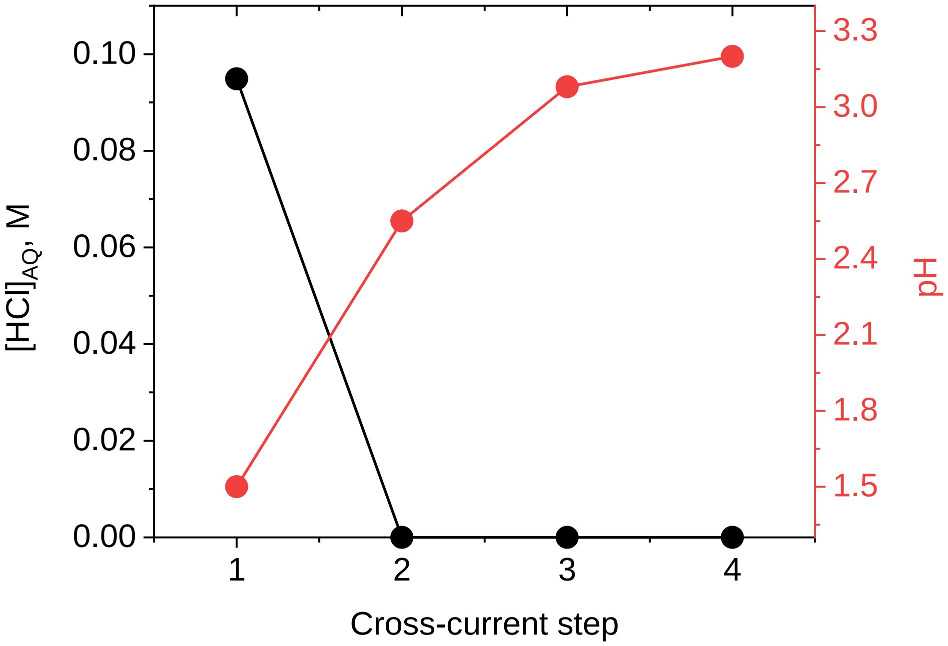

**Figure 29.** Evolution of HCl concentration and pH during a 4-stage cross-current extraction by 50 vol% TEHA. Conditions: $[HCl]_A$ = 0.52 mol $L^{-1}$, organic phase: 50 vol% TEHA + 5 vol% 1-decanol in D70 diluent, 500 rpm, 1h, room temperature, O:A = 3:1.

This project has received funding from the European Union's EU
Framework Programme for Research and Innovation Horizon
Europe under Grant Agreement No 101058124
https://enicon-horizon.eu/

**Figure 30.** Picture of the extraction experiment upon the formation of the precipitate.

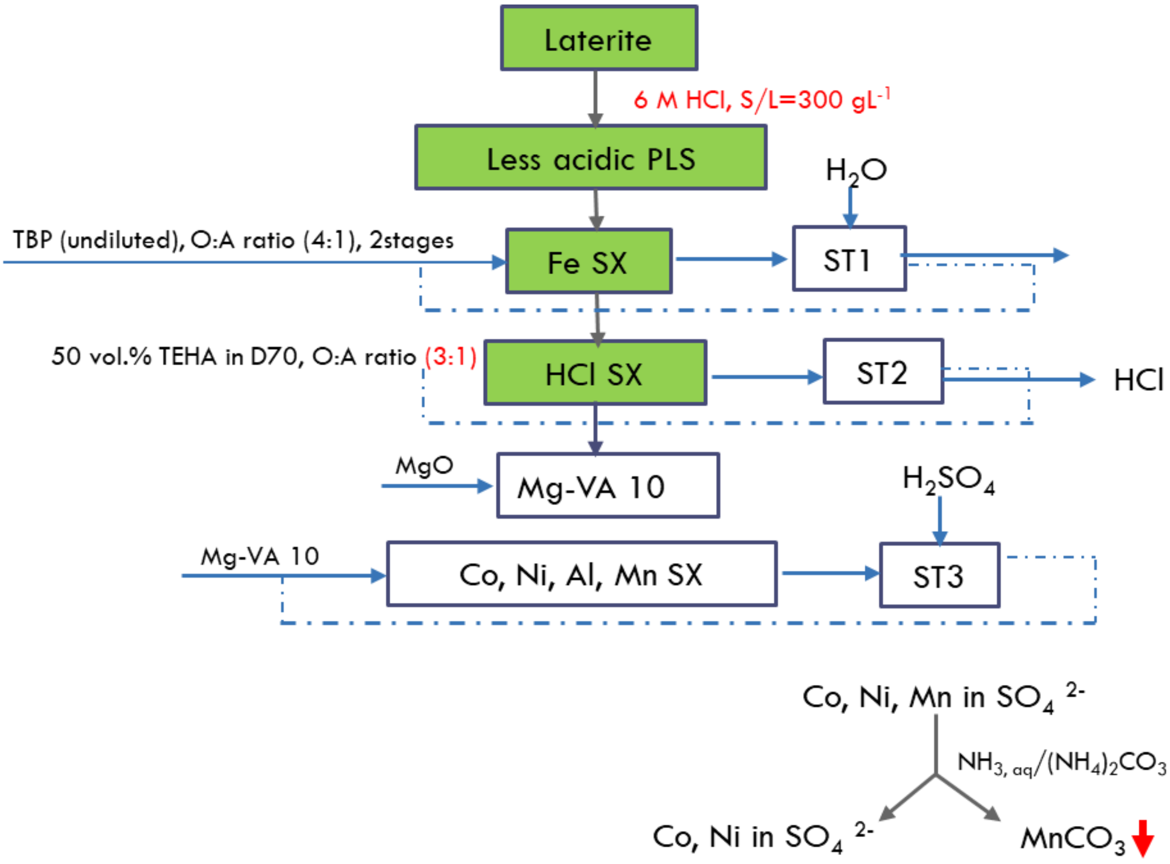

**Figure 31.** Preliminary flowsheet for the processing limonite (ENICON017) and saprolite (ENICON028) to obtain a pure Ni/Co solution using the ENICON HCl-based process. Some adjustments might still be required to optimise the Co, Ni, Mn extraction step with Versatic Acid 10. (SX = solvent extraction, ST = stripping, VA 10 = Versatic Acid 10)

This project has received funding from the European Union's EU Framework Programme for Research and Innovation Horizon Europe under Grant Agreement No 101058124
https://enicon-horizon.eu/

### 6.3.3 MHP and MSP

In order to purify the MHP and MSP intermediates, the remaining impurities should be removed from the PLS (Table 10) by solvent extraction. These impurities are the main issue for downstream processing, taking into account the compatibility with Nikkelverk's chlorine-route to obtain battery-grade cobalt and nickel. Concentrations in the MHP PLS are significantly higher than in the MSP PLS, due to differences in leaching conditions, i.e. the S/L ratio for MHP was 360 g $L^{-1}$ (ENICON013) and for MSP it was 50 g $L^{-1}$. This brings about a few consequences. For instance, in the case of MHP, it would not make sense to extract all Co(II) and Ni(II) by Versatic Acid 10, seen the high concentration of these metals. Instead, opting for the removal of Fe(III), and most of the Al(III) and Zn(II) by TBP, followed by the selective removal of Mg(II), Ca(II) and Mn(II) by D2EHPA would be a better choice. This preliminary flowsheet is presented in Figure 32. As this deviates from the original workplan, it was chosen to focus first on the optimisation of the MSP flowsheet instead (Figure 33). Here, the removal of Fe(III) and excess HCl were the most important, and these are results which can be easily replicated in the MHP leachate. Excess acid removal might not be necessary in MHP leachate, seen the low free acid concentration in the MHP PLS. As to the MSP PLS, the concentration of the other impurities besides Fe(III) were very low. Hence, there were no tests conducted to remove these impurities.

**Table 10.** Composition of the MHP and MSP PLS.

| | | g $L^{-1}$ | | | | | | | | | mol $L^{-1}$ |
|---|---|---|---|---|---|---|---|---|---|---|---|
| **Sample type** | **Code** | **Co** | **Ni** | **Fe** | **Mn** | **Al** | **Mg** | **Ca** | **Si** | **Zn** | **HCl** |
| **MHP** | 013 | 4.8 | 105.2 | 0.7 | 2.0 | 1.6 | 0.6 | 0.1 | 0.5 | 0.5 | <0.01 |
| **MSP** | 014 | 0.9 | 22.1 | 0.4 | - | - | 0.04 | - | - | 0.3 | 4.2 |

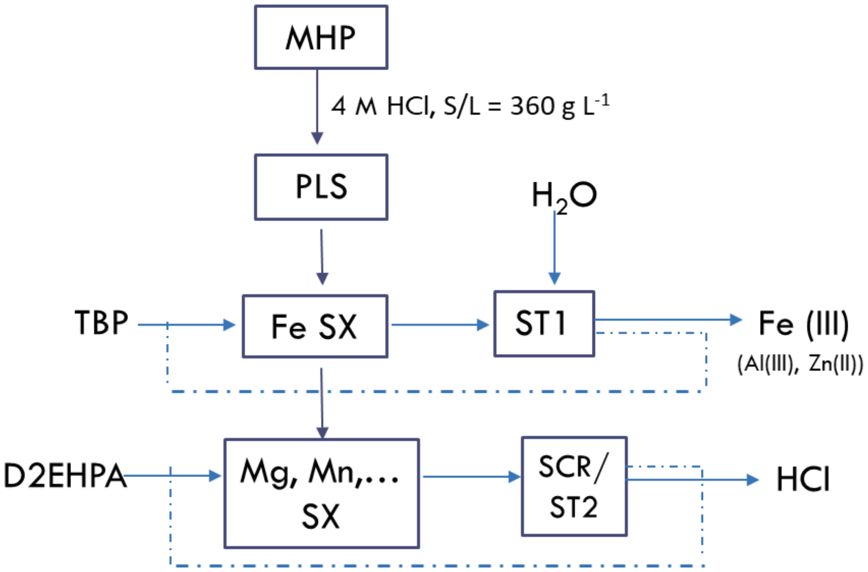

**Figure 32.** Preliminary flowsheet for the processing MHP to obtain a pure Ni/Co solution using the ENICON HCl-based process. Fe(III) solvent extraction parameters from the MSP process could be used for processing the MHP PLS as well, yet replication tests are still to be conducted. (SX = solvent extraction, ST = stripping)

This project has received funding from the European Union's EU Framework Programme for Research and Innovation Horizon Europe under Grant Agreement No 101058124
https://enicon-horizon.eu/

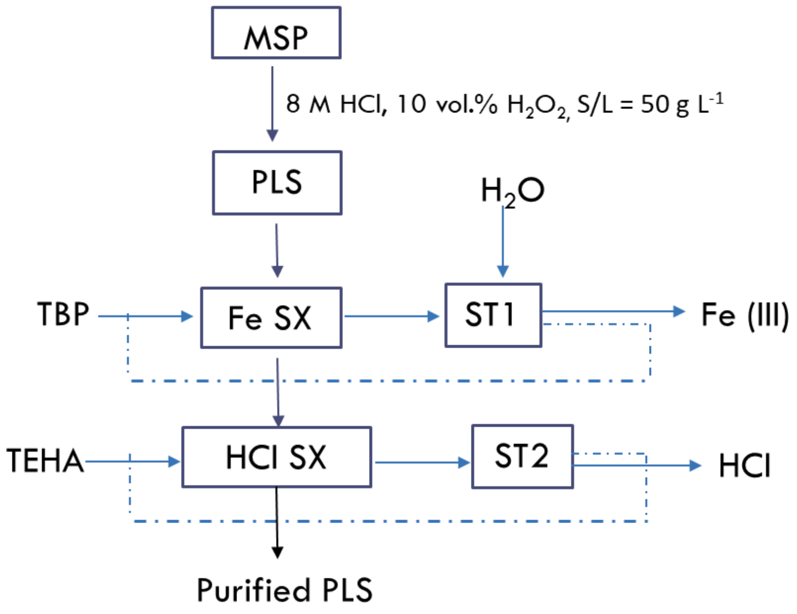

**Figure 33.** Preliminary flowsheet for the processing MSP to obtain a pure Ni/Co solution using the ENICON HCl-based process. (SX = solvent extraction, SCR = scrubbing, ST = stripping)

Since the Fe(III) concentration in the MSP PLS is very low, lower TBP concentrations should be investigated, as the use of undiluted TBP cannot be justified. Instead, all Fe(III) is extracted from the PLS using only 0.075 mol $L^{-1}$ TBP (Figure 34) Choosing a somewhat higher TBP concentration allows to choose lower O:A ratios, and would increase the final Fe(III) concentration in the strip solution. Indeed, as shown in Figure 35, all Fe(III) is extracted at the highest tested O:A ratio, i.e. 1:5, at [TBP] = 0.2 mol $L^{-1}$. It is possible to further optimise this, by choosing even lower O:A ratios or lower TBP concentrations.

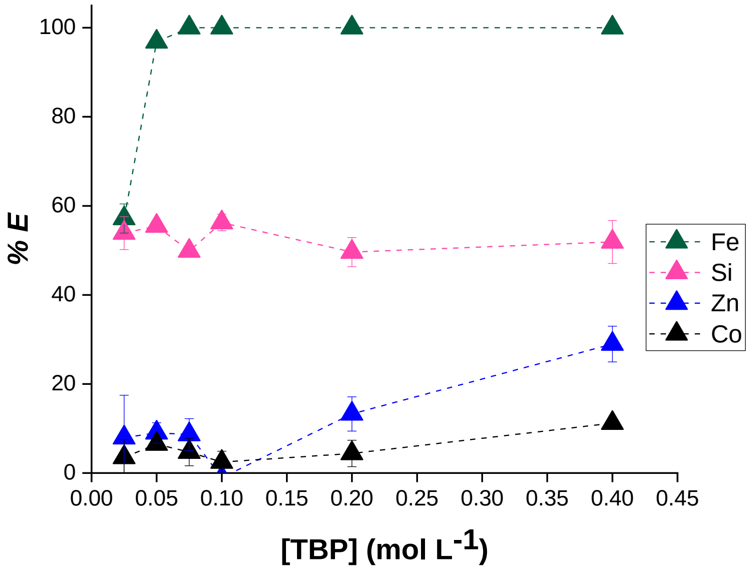

**Figure 34.** Effect of TBP concentration on the extraction of Fe(III) and other metals present in MSP PLS. Conditions: $[HCl]_A$ = 4.2 mol $L^{-1}$, organic phase: 0.01 – 0.4 mol $L^{-1}$ TBP + 5 vol% 1-decanol in D70 diluent, 500 rpm, 15 min, room temperature, O:A = 1:1.

This project has received funding from the European Union's EU Framework Programme for Research and Innovation Horizon Europe under Grant Agreement No 101058124
https://enicon-horizon.eu/

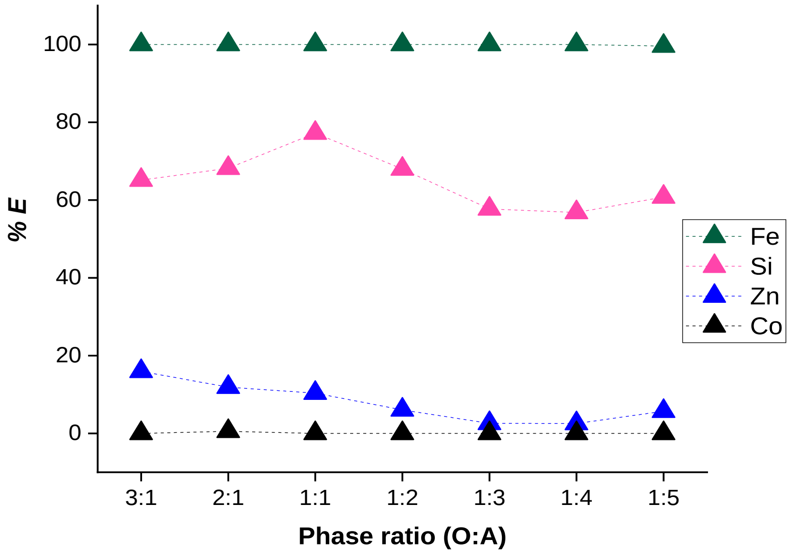

**Figure 34.** Effect of the organic-to-aqueous phase ratio (O:A) on the extraction of Fe(III) and other metals present in MSP PLS. Conditions: $[HCl]_A$ = 4.2 mol $L^{-1}$, organic phase: 0.2 mol $L^{-1}$ TBP + 5 vol% 1-decanol in D70 diluent, 500 rpm, 15 min, room temperature.

After the 1-stage removal of Fe(III), the free acid in the MSP PLS should be recovered. The concentration of HCl is very high compared to the concentration of TEHA in the organic phase, i.e. 40 vol% or about 0.9 mol $L^{-1}$. No higher TEHA concentrations were investigated, due to viscosity issues. Hence, a O:A ratio of at least 5:1 would be necessary to extract all HCl from the PLS. This is reflected in Figure 35: the extraction efficiency is only about 10% at O:A = 1:1, while it increases to 70% at 5:1 and almost 100% at 9:1. Note that the co-extraction of Co(II) decreases greatly at higher O:A ratios. Multi-stage counter-current extraction might improve the extraction efficiency at O:A = 5:1, and reduce the co-extraction of Co(II) as well. Stripping is still to be investigated. The maximum HCl concentration after stripping, however, would only be 0.9 mol $L^{-1}$, i.e. the concentration of TEHA. Further up-concentration would be necessary to re-use this for leaching, yet this is a big energy cost.

This project has received funding from the European Union's EU Framework Programme for Research and Innovation Horizon Europe under Grant Agreement No 101058124
https://enicon-horizon.eu/

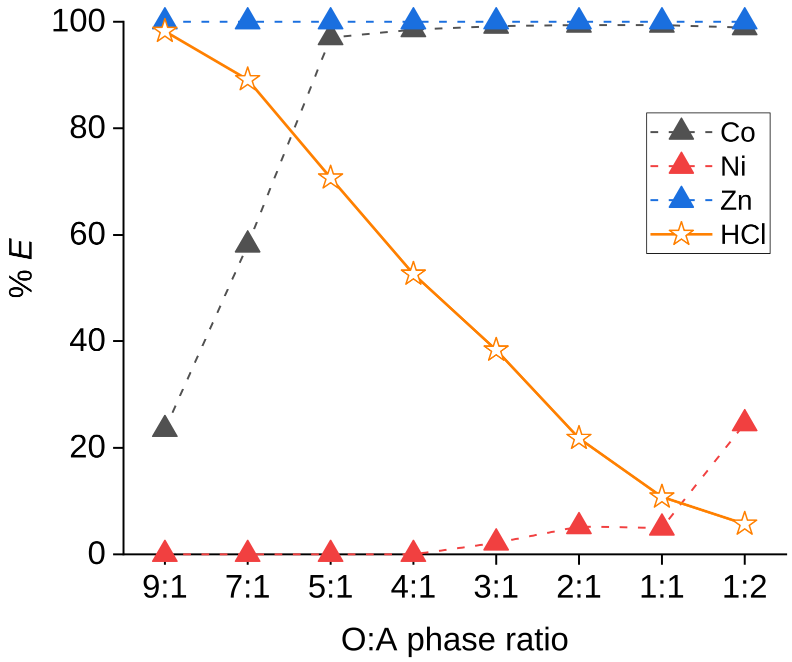

**Figure 35.** Effect of the organic-to-aqueous phase ratio (O:A) on the extraction of HCl and metals present in MSP PLS. Conditions: $[HCl]_A$ = 4.2 mol $L^{-1}$, organic phase: 40 vol% TEHA in A150 diluent, 500 rpm, 15 min, room temperature.

### 6.4 *Hydrolytic distillation*

Currently, HCl can be recovered using costly and energy-intensive pyrohydrolysis. This process converts the obtained metal chloride solution back to hydrochloric acid and metal oxides at a temperature up to 850 °C. An alternative process has been developed that can distil HCl from a solution containing iron and/or magnesium chloride at a much lower temperature (± 200 °C). Although promising, further research is needed to optimise the process and try it on different metal chloride streams.

A thorough chemical understanding of the process will help to reveal the possibilities of challenges. A thermodynamic model is indispensable for this. It allows investigating the chemistry at highly non-ideal conditions, where activities are more suited than molar concentrations. Such a thermodynamic model can also boost the applicability of hydrolytic distillation for hydrochloric acid recovery in metallurgical processes because it helps the calculation of the optimal conditions. This avoids a troublesome and time-consuming experimental campaign every time the initial composition of the metal chloride solution changes.

A hydrolytic distillation with 200 mL of 4 mol $L^{-1}$ $FeCl_3$ showed that superazeotropic HCl can be produced at a boiling temperature above 180 °C (Figure 36). The overall reaction equation is as follows:

$$2\mathrm{FeCl}_{3,\mathrm{aq}} + 3\mathrm{H}_2\mathrm{O} \rightleftharpoons \mathrm{Fe}_2\mathrm{O}_{3,\mathrm{s}} + 6\mathrm{HCl}_\mathrm{g} \qquad (6)$$

The gas temperature at the condenser inlet was between 100 and 130 °C, and the highest HCl concentration in the condensate was 10.7 mol $L^{-1}$ at a boiling liquid temperature of 187 °C. Water was added to the boiling flask to keep the temperature between 180 and 195 °C and to ensure that the system did not run dry.

This project has received funding from the European Union's EU
Framework Programme for Research and Innovation Horizon
Europe under Grant Agreement No 101058124
https://enicon-horizon.eu/

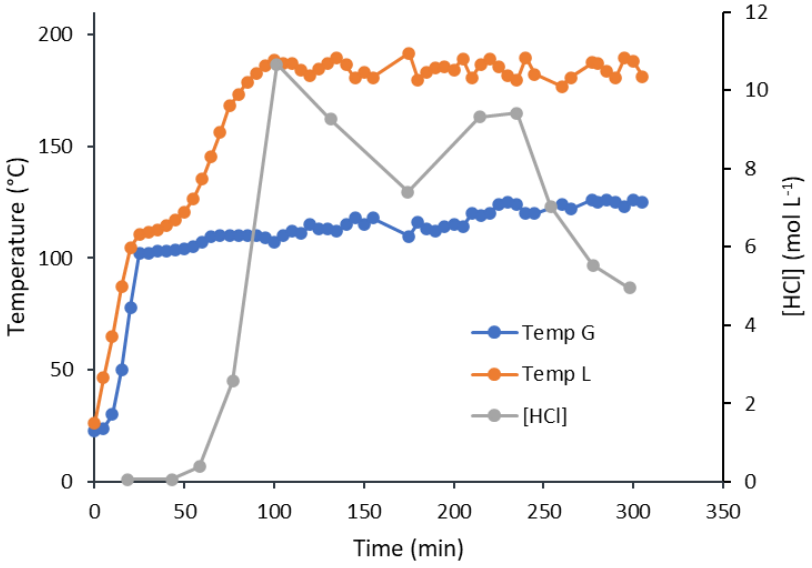

**Figure 36.** Hydrolytic distillation of 4 mol L$^{-1}$ $FeCl_3$ with periodic water addition. Temp G is the temperature of the gas phase at the top of the distillation setup, Temp L is the boiling flask liquid temperature, and [HCl] is the concentration of HCl in the concentrate.

OLI Studio (OLI Systems Inc., Parsippany NJ) with the MSE and Geochem databases was used to calculate this system. The Geochem sub-database was used because it includes hematite, formed in longer timeframes or at higher temperatures. Experimental observations also confirm the formation of hematite in similar systems.[9] OLI Systems provides thermodynamic software, meaning that the equilibrium compositions and other aspects of the equilibrium can be calculated in function of temperature, pressure, and initial composition. The time dependence of the distillation cannot be included in the calculations as heat and mass transfer equations, and kinetic parameters are not included in OLI. Thus OLI can calculate the formation of HCl at a certain temperature and initial composition, but not how long it takes to convert the initial feed to the metal oxide and HCl.

OLI calculates a maximum concentration of HCl in the condensate that equals the highest concentration observed in the experiment (Figure 37). However, OLI calculates HCl distillation already at lower temperatures of the liquid in the boiling flask compared to the experiment. Probably, the experimental temperature difference between the boiling flask (± 180 °C) and the gas phase at the inlet of the condenser (± 120 °C) explains the difference with the OLI calculation. OLI calculates the systems as if all parts are at the same temperature. Based on this analysis, it would be better to calculate the onset of HCl distillation based on the temperature of the gas at the inlet of the condenser.

A distillation of 4 mol L$^{-1}$ $AlCl_3$ did not produce HCl at the boiling point (120 °C) of the solution, but a mixture of 4 mol L$^{-1}$ $MCl_3$ (90 % Fe and 10% Al) did produce HCl above 180 °C in the boiling flask.

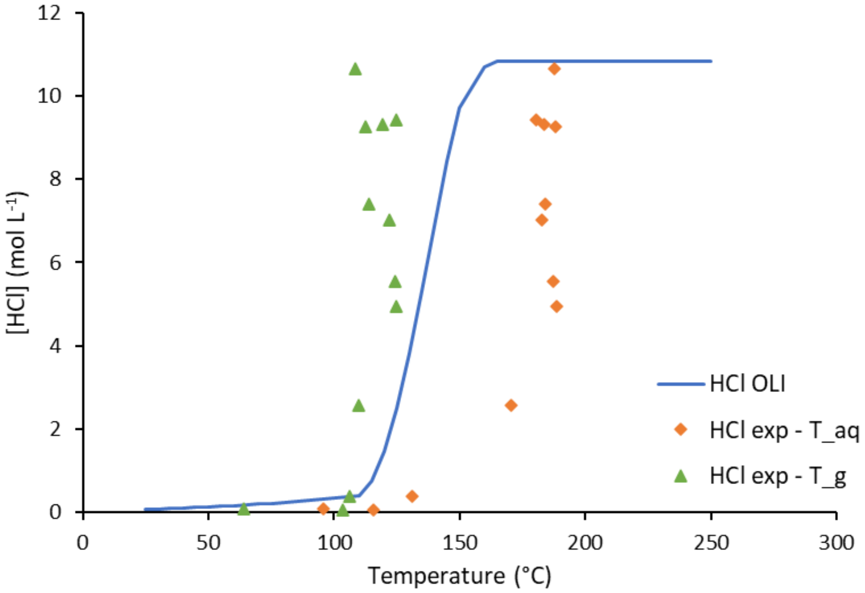

***Figure 37.*** *OLI Studio calculation and experimental results for the concentration of HCl in the condensate at different temperatures of the boiling solution (T_aq) and of the gas just before the inlet of the compensator (T_g).*

## *6.5 SX-assisted carbonation*

During acid leaching, protons are consumed either through the reaction of the acid with solid particles or by neutralising the excess acid with a base after leaching, which increases the pH for solution purification. As long as the acid anions remain in the system, the acid can be regenerated by reintroducing the consumed protons to the system by, for example, introducing hydrogen gas or by oxidising water molecules.[10,11] Alternatively, carbon dioxide gas ($CO_2$) represents an inexpensive and safe technology that can provide sufficient protons indirectly through the reaction with water, allowing also the formation of valuable metal carbonates. This approach can be coupled with acid extraction by solvent extraction, so that the precipitation of carbonate compounds can be promoted in the acid-free aqueous phase. While $MgCl_2$ and $CaCl_2$ are the main focus within ENICON for the recovery of HCl through SX-assisted carbonation, seen the prevalence of these in laterite PLS, it was chosen to start the optimisation experiments for LiCl. Moreover, these results might be useful when, for instance, replicating the ENICON process to the recycling of lithium-ion battery black mass. The results below focus in the carbonation of lithium from a synthetic solutions containing 245 g $L^{-1}$ of LiCl. The lithium conversion was evaluated during the extraction/carbonation stage by considering different O:A-ratios, while 1-octanol and Shellsol D70 were evaluated as diluents.

### *6.5.1 Exploration of different extractants in the presence of Shellsol D70 as diluent for lithium conversion*

Figure 38a describes the lithium conversion yield obtained in the presence of TEHA, $T_{iso}$OA and TOA as extractants. The highest lithium conversion yield was achieved with 50 vol% TOA, as this tends to have much higher basicity than TEHA and $T_{iso}$OA. Note that amine-based extractants can function as catalysts to enhance the hydration of $CO_2$ molecules into $H_2CO_3$, as described in Equation 7, which reaction rate is favoured in the presence of highly basic amines. Therefore, in the presence of less basic extractants, the hydration of $CO_2$ molecules is less efficient, limiting the amount of carbonate ions available for carbonation. As can be observed in Figure 38b, no solid particles were visible during phase separation of mixtures containing TEHA

This project has received funding from the European Union's EU Framework Programme for Research and Innovation Horizon Europe under Grant Agreement No 101058124
https://enicon-horizon.eu/

and $T_{iso}OA$. This could indicate that lithium could have been converted into $LiHCO_3$, which is highly soluble, rather than into $Li_2CO_3$.

$$H_2O_{(l)} + CO_{2(aq)} + \overline{NR_3}_{(org)} \leftrightarrow \overline{R_3NH^+}_{(org)} + HCO^-_{3(aq)} \tag{7}$$

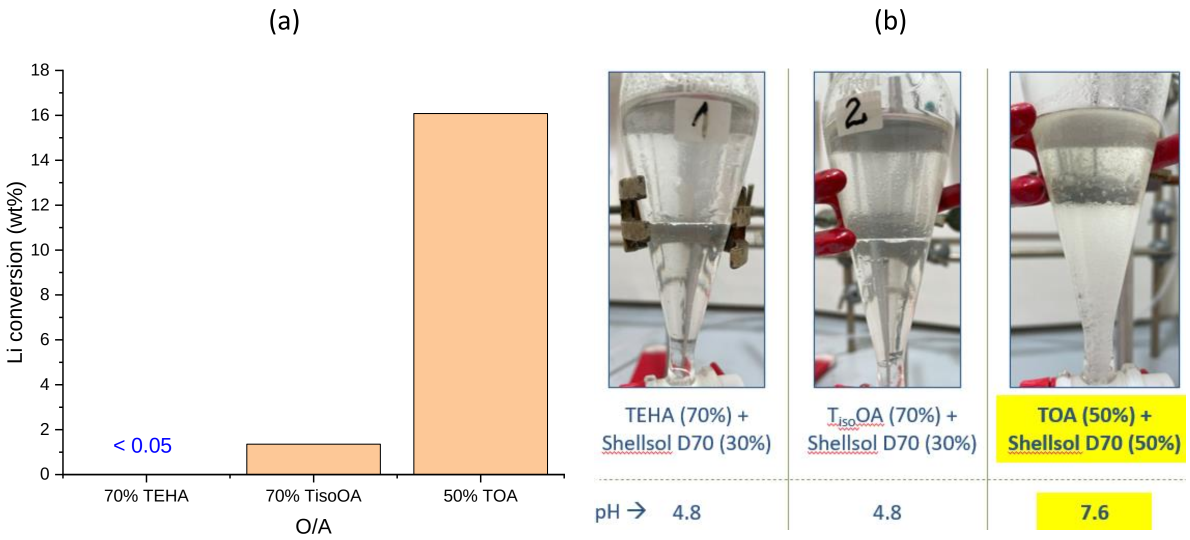

**Figure 38.** (a) Effect of different extractants on lithium conversion with Shellsol D70 as diluent. (b) Photograph of the different solutions (containing both aqueous and organic phases) in the corresponding separation funnel (pH values of the aqueous phases are also shown)

Figure 39 shows the effect of different mixtures of TOA and Shellsol D70 on lithium conversion and pH. Lithium conversion increases when increasing the O:A ratio (Figure 39a), particularly when a concentration between 50–70 vol% of TOA is used. Yet, the highest conversion yield was only about 15 wt%. The low conversion yield was caused by the relatively low pH values attained during the extraction/carbonation experiments, ranging between 5.0 and 7.0, which just in few cases was above 6.0, i.e. above the threshold for carbonation. Based on these results, TOA was chosen as the most optimal extractant to be considered for further studies.

This project has received funding from the European Union's EU Framework Programme for Research and Innovation Horizon Europe under Grant Agreement No 101058124
https://enicon-horizon.eu/

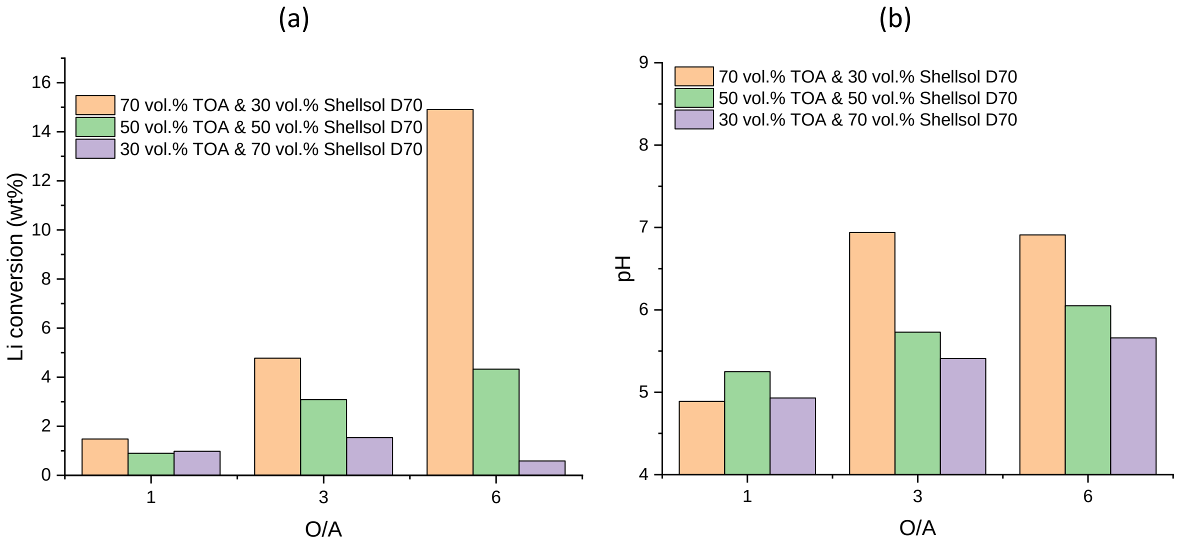

**Figure 39.** Effect of TOA and Shellsol D70 concentration on (a) pH of the aqueous phase and (b) lithium conversion.

### *6.5.2 Lithium conversion in the presence of TOA and 1-octanol.*

Figure 40 describes the lithium conversion and the pH of the aqueous phase obtained after extraction/carbonation, with different O:A ratios, using TOA as extractant and 1-octanol as diluent. Relatively high lithium conversion was achieved when the initial lithium concentration was 40 g $L^{-1}$. Lower initial lithium concentration than that of 40 g $L^{-1}$ did not favour carbonation (Figure 40a). The pH of the aqueous phase was in all cases above 6.0 (Figure 40b).

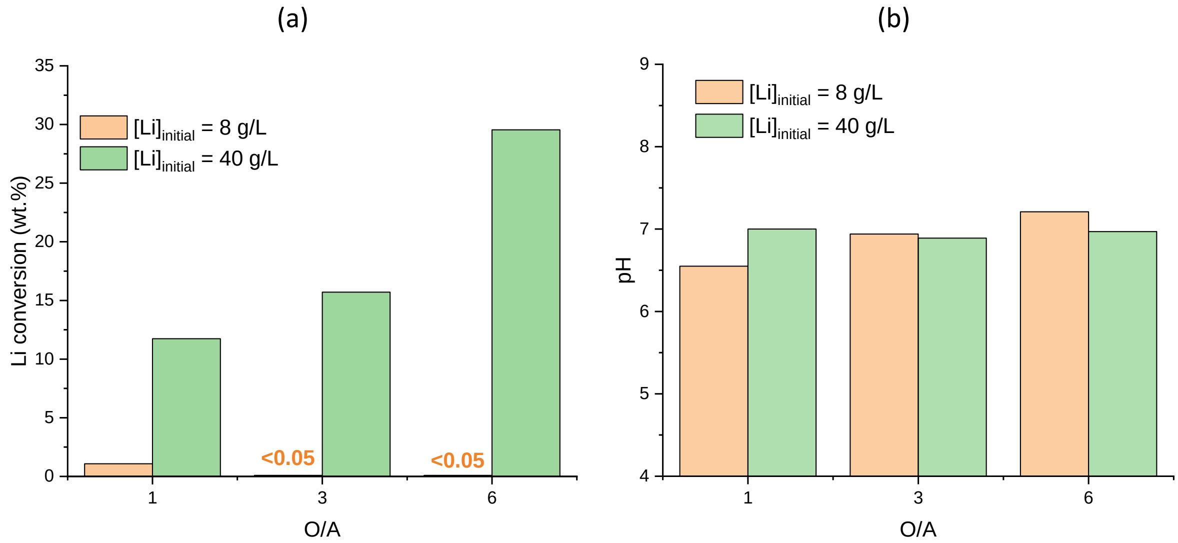

**Figure 40.** Effect of initial lithium concentration on (a) lithium conversion and (b) pH of aqueous phase after extraction/carbonation using different O:A-ratios. The organic phase was composed of 70 vol% TOA and 30 vol% 1-octanol.

The mineralogical composition of the carbonate product obtained after extraction/carbonation was analysed by XRD. Figure 41 shows the XRD pattern of the solid product obtained from the LiCl solution after extraction/carbonation (with an O:A ratio of 6) in the presence of TOA and 1-octanol. The obtained solid product correspond to a highly pure lithium carbonate compound.

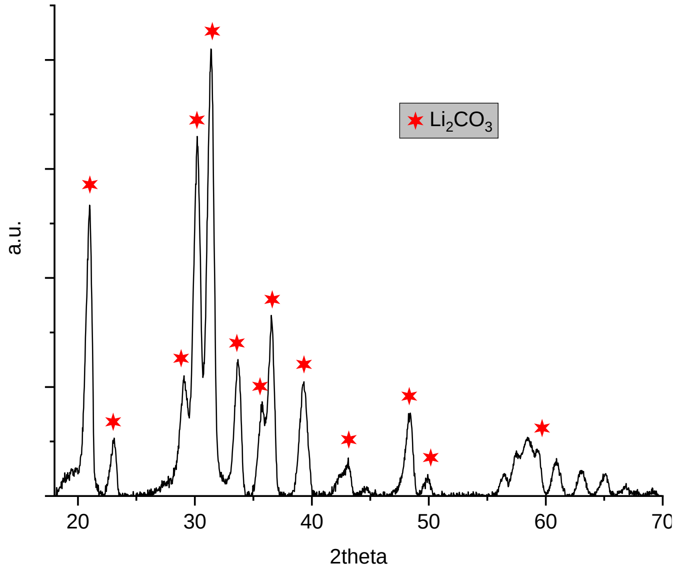

**Figure 41.** XRD pattern of the solid product obtained after extraction/carbonation with an O:A-ratio of 6 in the presence of 70 vol% TOA and 30 vol% 1-octanol. The initial lithium concentration was about 40 g $L^{-1}$.

### *6.5.3 Hydrochloric acid extraction and regeneration*

The chloride concentration was determined in the corresponding aqueous solution obtained after extraction/carbonation and stripping by titration with 0.05 mol $L^{-1}$ $AgNO_3$ as titer. A synthetic solution with 244 g $L^{-1}$ of LiCl (i.e. 40 g $L^{-1}$ of Li) was considered in these experiments, and the mixture of TOA (70 vol%) with 1-octanol (30 vol%) was used as the organic phase. As described in Table 11, the extraction/carbonation stage was carried out with three different O:A ratios, i.e. 1, 3 and 6. Stripping for HCl regeneration (determined indirectly from the $Cl^-$ concentration) was conducted with milli-Q water at 60 ˚C and a constant O:A ratio of 0.3.

**Table 11.** Conditions for obtaining the corresponding aqueous solutions from extraction/carbonation and stripping.

| **Aqueous solution** | **O:A ratios** | |
|---|---|---|
| | **Extraction/Carbonation** | **Stripping** |
| I | 1 | 0.3 |
| II | 3 | 0.3 |
| III | 6 | 0.3 |

Figure 42 describes the corresponding extraction (into the organic phase during the extraction/carbonation stage) and regeneration (through stripping) yields of hydrochloric acid. The amount of acid extracted into the organic phase increases when increasing the O:A ratio, as the highest extraction yield was approximately 28% of HCl with a O:A ratio of 6, but the regeneration of the acid resulted less efficient as less than 1% of the acid was recovered. On the other hand, when less acid was extracted into the organic phase (about 7.7%) – with an O:A ratio of 1 during the extraction/carbonation stage – about 10% of the acid was effectively regenerated from the loaded organic phase.

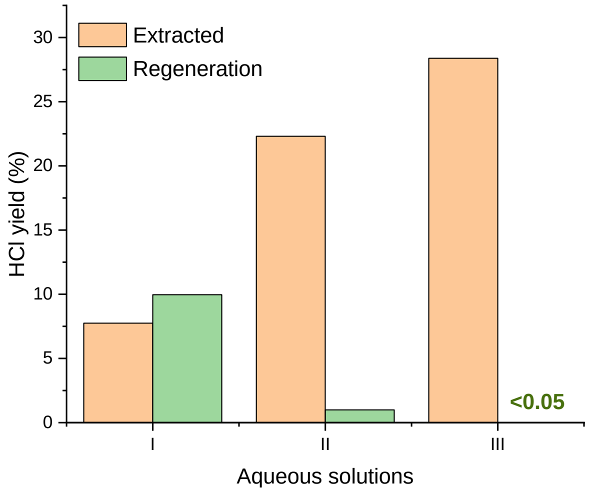

**Figure 42.** Extraction and regeneration yields of hydrochloric acid from aqueous solution obtained after extraction/carbonation and stripping, respectively. The description of the corresponding aqueous solutions is presented in Table 11.

This project has received funding from the European Union's EU
Framework Programme for Research and Innovation Horizon
Europe under Grant Agreement No 101058124
https://enicon-horizon.eu/

# 7 Conclusions

Present report describes a novel approach for the recovery of cobalt and nickel from five selected (European) materials: ferronickel, limonitic and saprolitic laterite, MHP and MSP. Optimisation of the process parameters of the new HCl-based process is largely completed, and involved the leaching , three-tier solvent extraction (iron removal, HCl recovery and Ni/Co recovery), hydrolytic distillation and SX-assisted carbonation. Thermodynamic modeling provided the necessary support for the optimisation work. Below is a list with the most important conclusions for each process step:

- Leaching was performed at ambient pressure and low temperature (< 100 °C), resulting in high recoveries of cobalt and nickel: ≥ 86% for cobalt, ≥ 94% for nickel.
- Extraction of Fe(III) by TBP worked well for all material streams. Moreover, for the leach solutions having high Fe(III) concentrations (ferronickel, laterites), simultaneous recovery of HCl is possible, if leaching conditions are adjusted to obtain close to equimolar quantities of Fe(III) and HCl. In other cases, TEHA is to be used to quantitatively extract excess HCl and to adjust the initial pH of the aqueous solution before extraction of nickel and cobalt by Versatic Acid 10. This last extraction step is still under investigation, as precipitation occurred during solvent extraction experiments at higher pH.
- Hydrolytic distillation of a synthetic $FeCl_3$ solution regenerated a HCl solution with a concentration of 10.7 mol $L^{-1}$. This work is to be replicated in the next months using a real solution, containing about 0.7 mol $L^{-1}$ $FeCl_3$ as well as 1 mol $L^{-1}$ free HCl.
- Proof-of-principle tests show that the SX-assisted carbonation of LiCl can be performed in concentrated solutions (≥ 40 g $L^{-1}$ Li). Still, yields are relatively low (< 30%) and the recovery of the extracted acid is troublesome. This is currently being replicated for $MgCl_2$ and $CaCl_2$, yet the low concentrations of these salts in the laterite PLSs might be a limiting factor for the applicability of this approach.

As to the KPI's mentioned earlier, an estimation of the purity of a theoretical MHP product obtained from quantitative hydroxide precipitation can be calculated for a raffinate obtained after Fe(III) and HCl removal from ferronickel PLS. This calculation resulted in a Ni/Co purity of 55.7%, with calcium and iron hydroxides as main impurities. This is significantly higher than the 42% purity envisioned for MHP as KPI.

Upscaling efforts, starting December 2024 (M31), will primarily focus on the three most promising routes. Based on the the five material flowsheets, an overview was made for the technical feasibility to upscale the process and obtain a pure Ni/Co solution (Table 12). Although a few more optimisation studies might be needed, ferronickel (ENICON023), limonitic laterite (ENICON017) and saprolitic laterite (ENICON028) seem to be the most promising, as (1) all these materials have shown excellent recovery of cobalt and nickel using HCl solutions, (2) the main impurity, Fe(III), is present in larger quantities and can easily be removed together with most of the excess HCl, thus improving the feasibility for HCl recovery, and (3) most of these materials are available in larger amounts. Some further optimisations would be needed for the separation of cobalt and nickel from Mn(II), Mg(II), Ca(II) and Al(III) impurities from laterite solutions. These conclusions will make up the decision described in Milestone 11 (m2.2) *Selection of 3 most appropriate (cf. TEA) ENICON input streams for further process integration & validation in T2.3.5 (candidates: FeNi product, Ni laterites, Ni/Co-sulphide concentrate, MHP/MSP from pyrite tailings, carbonated Ni-silicate tailings).*

**Table 12.** Overview of the technical feasibility for the scale-up of ENICON flowsheets

| | ferronickel | limonite | saprolite | MHP | MSP |
|---|---|---|---|---|---|
| Leaching efficiency | high recoveries of cobalt and nickel using mild conditions | high recoveries of Co(II) and nickel using mild conditions | high recoveries of Co(II) and nickel using mild conditions | high recoveries of Co(II) and nickel using mild conditions | Harsher conditions, lower S/L ratios needed for efficient recovery cobalt of and nickel |
| Impurities management | Easy removal of impurities, limited losses cobalt and nickel | Impurity removal complicated | Impurity removal complicated | Impurity removal complicated | Easy removal of impurities, limited losses cobalt and nickel |
| Materials availability | Plenty available | Plenty available | Plenty available | Limited availability | Limited availability |
| feasibility for improving circularity | Improvement circularity through simultaneous recovery of excess HCl and $FeCl_3$ | Improvement circularity through simultaneous recovery of excess HCl and $FeCl_3$ | Improvement circularity through simultaneous recovery of excess HCl and $FeCl_3$ | Improvement circularity limited to potential recovery of HCl from low concentration of $MgCl_2$ and $CaCl_2$ | Presence of sulphates and high excess of HCl concentration complicates circularity |

This project has received funding from the European Union's EU Framework Programme for Research and Innovation Horizon Europe under Grant Agreement No 101058124
https://enicon-horizon.eu/

# 8 References

(1) Binnemans, K.; Jones, P. T. The Twelve Principles of Circular Hydrometallurgy. *J. Sustain. Metall.* **2022**, *9* (1), 1–25. https://doi.org/10.1007/s40831-022-00636-3.

(2) Kyle, J. H. Nickel Laterite Processing Technologies – Where to Next? In *ALTA 2010 Nickel/Cobalt/Copper Conference*; Perth, Western Australia, **2010**.

(3) IEA. *The Role of Critical Minerals in Clean Energy Transitions*; **2021**. https://www.iea.org/reports/the-role-of-critical-minerals-in-clean-energy-transitions.

(4) Bartzas, G.; Komnitsas, K. Cradle to Gate Life-Cycle Assessment of Battery Grade Nickel Sulphate Production through High-Pressure Acid Leaching. *Sci. Total Environ.* **2024**, *952* (September), 175902. https://doi.org/10.1016/j.scitotenv.2024.175902.

(5) Wang, P.; Anderko, A.; Young, R. D. A Speciation-Based Model for Mixed-Solvent Electrolyte Systems. *Fluid Phase Equilib.* **2002**, *203* (1–2), 141–176. https://doi.org/10.1016/S0378-3812(02)00178-4.

(6) Wang, P.; Anderko, A.; Springer, R. D.; Young, R. D. Modeling Phase Equilibria and Speciation in Mixed-Solvent Electrolyte Systems: II. Liquid–Liquid Equilibria and Properties of Associating Electrolyte Solutions. *J. Mol. Liq.* **2006**, *125* (1), 37–44. https://doi.org/10.1016/j.molliq.2005.11.030.

(7) Lommelen, R.; Binnemans, K. Molecular Thermodynamic Model for Solvent Extraction of Mineral Acids by Tri-n-Butyl Phosphate (TBP). *Sep. Purif. Technol.* **2023**, *313*. https://doi.org/10.1016/j.seppur.2023.123475.

(8) Lommelen, R.; Dewulf, B.; Bussé, J.; Binnemans, K. Predictive Thermodynamic Model for Solvent Extraction of Iron(III) by Tri-n-Butyl Phosphate (TBP) from Chloride Media. *Sep. Purif. Technol.* **2024**, *348*. https://doi.org/10.1016/j.seppur.2024.127708.

(9) Becze, L.; Hock, S. J.; Demopoulos, G. P. Precipitation of Hematite and Recovery of Hydrochloric Acid from Concentrated Iron Chloride Solutions by a Novel Hydrolytic Decomposition Process. In *EPD Congress 2011*; Wiley, **2011**; pp 529–538. https://doi.org/10.1002/9781118495285.ch60.

(10) Agrawal, A.; Kumar, V.; Pandey, B. D.; Sahu, K. K. A Comprehensive Review on the Hydro Metallurgical Process for the Production of Nickel and Copper Powders by Hydrogen Reduction. *Mater. Res. Bull.* **2006**, *41* (4), 879–892. https://doi.org/10.1016/j.materresbull.2005.09.028.

(11) Schmachtel, S.; Toiminen, M.; Kontturi, K.; Forsén, O.; Barker, M. H. New Oxygen Evolution Anodes for Metal Electrowinning: MnO2 Composite Electrodes. *J. Appl. Electrochem.* **2009**, *39* (10), 1835–1848. https://doi.org/10.1007/s10800-009-9887-1.